BUCKLING OF CYLINDRICAL METAL SHELLS RESTING ON DISCRETELY SUPPORTED RING BEAMS

A THESIS SUBMITTED TO
THE GRADUATE SCHOOL OF NATURAL AND APPLIED SCIENCES
OF
MIDDLE EAST TECHNICAL UNIVERSITY

BY

CEM SONAT

IN PARTIAL FULFILLMENT OF THE REQUIREMENTS
FOR
THE DEGREE OF MASTER OF SCIENCE
IN
CIVIL ENGINEERING

AUGUST 2013

Approval of the thesis:

BUCKLING OF CYLINDRICAL METAL SHELLS RESTING ON DISCRETELY SUPPORTED RING BEAMS

submitted by **CEM SONAT** in partial fulfillment of the requirements for the degree of **Master of Science in Civil Engineering Department, Middle East Technical University** by,

Prof. Dr. Canan Özgen _____
Dean, Graduate School of **Natural and Applied Sciences**

Prof. Dr. Ahmet Cevdet Yalçıner _____
Head of Department, **Civil Engineering**

Prof. Dr. Cem Topkaya _____
Supervisor, **Civil Engineering Dept., METU**

Examining Committee Members:

Assoc. Prof. Dr. Afşin Sarıtaş _____
Civil Engineering Dept., METU

Prof. Dr. Cem Topkaya _____
Civil Engineering Dept., METU

Asst. Prof. Dr. Serdar Göktepe _____
Civil Engineering Dept., METU

Asst. Prof. Dr. Ercan Gürses _____
Aerospace Engineering Dept., METU

Asst. Prof. Dr. Eray Baran _____
Civil Engineering Dept., Atılım University

Date: August 1, 2013

I hereby declare that all information in this document has been obtained and presented in accordance with academic rules and ethical conduct. I also declare that, as required by these rules and conduct, I have fully cited and referenced all material and results that are not original to this work.

Name, Last name: Cem, Sonat

Signature:

ABSTRACT

BUCKLING OF CYLINDRICAL METAL SHELLS RESTING ON DISCRETELY SUPPORTED RING BEAMS

Sonat, Cem
M.Sc., Department of Civil Engineering
Supervisor: Prof. Dr. Cem Topkaya

August 2013, 64 pages

Silos in the form of cylindrical metal shells can be supported by evenly spaced columns in applications where an access space is needed for discharge of contained solids. In large silos a ring beam is utilized to more evenly distribute the column forces into the shell. The presence of discrete supports results in a non-uniformity of meridional stresses around the circumference. The stress non-uniformity must be taken into account in assessing the stability of the shell. Design standards provide recommendations for buckling of shells under uniform compression while being silent for providing solutions for non-uniform stresses. Designers have to resort to onerous finite element analysis which includes geometric and material nonlinearities with imperfections (GMNIA). A parametric study has been undertaken to develop a family of resistance curves which can be directly used in design without the need for complicated analysis. The resistance curves depend on the plastic resistance and elastic buckling resistance. Simple algebraic equations were developed to represent the plastic and elastic buckling resistances which were obtained using material nonlinear analysis (MNA) and linear bifurcation analysis (LBA), respectively. The proposed methodology is based entirely on hand calculations except for finding the degree of non-uniformity in the meridional stresses, which can be determined using linear finite element analysis.

Keywords: Cylindrical shells, buckling, ring beam, finite element analysis, silos

ÖZ

TEKİL MESNETLİ RİNG KİRİŞLERİ İLE DESTEKLENEN SİLİNDİR METAL KABUK YAPILARININ BURKULMASI

Sonat, Cem
Yüksek Lisans, İnşaat Mühendisliği Bölümü
Tez Yöneticisi: Prof. Dr. Cem Topkaya

Ağustos 2013, 64 sayfa

Silindir metal yapılardan olan silolar, uygulamalarda, içlerinde depolanan malzemelerin boşaltılabilmesi için altlarında bir ulaşım boşluğu bırakılarak, birbirinden eşit uzaklıktaki kolonlarla desteklenebilirler. Büyük silolarda kolon kuvvetlerini kabuğa daha eşit bir şekilde dağıtabilmek için ring kirişlerden faydalanılır. Tekil mesnetlerin varlığı silonun çevresindeki basınçların düzgün olmayan bir şekilde dağılmasına sebep olur. Kabukların sağlamlığını değerlendirirken bu düzgün olmayan basınç dağılımlarını da hesaba katmak gerekir. Tasarım standartları değişmeyen basınç altındaki kabukların burkulması konusunda önerilerde bulunurken, değişken basınç durumları için çözüm üretmek konusunda sessiz kalmaktadır. Tasarımcılar doğrusal olmayan geometrik ve malzeme özellikleri içeren ve kusurluluk içeren (GMNIA) külfetli sonlu elemanlar analizlerine başvurmak zorunda kalmaktadır. Karmaşık tahkiklere ihtiyaç duymaksızın direkt olarak kullanılabilecek bir takım dayanım eğrileri geliştirmek için parametrik bir çalışmaya girişilmiştir. Dayanım eğrileri, plastik dayanım ve elastik burkulma dayanımına bağlıdır. Sırasıyla doğrusal olmayan malzeme analizi (MNA) ve doğrusal çatallanma analizi (LBA) yapılarak elde edilen plastik ve elastik burkulma dayanımlarını temsil edecek basit cebirsel denklemler geliştirilmiştir. İleri sürülen yöntem doğrusal sonlu eleman analiziyle değişken basıncın mertebesini saptamak dışında tamamiyle el hesabına dayanmaktadır.

Anahtar Kelimeler: Silindir kabuklar, burkulma, ring kirişi, sonlu eleman analizi, silo

To the Future

ACKNOWLEDGMENTS

The author would like to express his deepest gratitude to his supervisor Prof. Dr. Cem Topkaya for his guidance, encouragements and motivation through the research and during the writing of the thesis. This work could never have been completed that much organized without Prof. Dr. Cem Topkaya's clarity and sagacity.

Special thanks go to Professor J. Michael Rotter for his guidance and advices.

The author also wants thank his colleagues and friends İlkay İhsan Önal, Alper Aldemir, Andaç Lüleç, Egemen Günaydın and İsmail Ozan Demirel for sharing their experiences throughout the author's master program and for their valuable friendship.

Lastly, the author wants to word his gladness to all members of the Water Resources Laboratory for the peaceful and respectful working environment. Especially Meriç Selamoğlu and Melih Çalamak are greatly appreciated for their sincere helps regarding to the author's assistantship work and for their precious friendship.

TABLE OF CONTENTS

LIST OF TABLES

TABLES

LIST OF FIGURES

FIGURES

CHAPTER 1

INTRODUCTION

1.1 General Information About Discretely Supported Silos

Cylindrical metal silos can be supported either on ground or on a few column supports, depending on the requirements of the discharge system. In cases where the granular solids contained within silos are discharged by gravity, a hopper is needed at the base with an access space beneath it to permit discharge into transportation systems. Most silos are supported on columns as shown in Figure 1.1 to provide this space. There are stringent limitations on the number of column supports that can be used because presence of columns does not allow for easy access by the transportation system. While a large number of columns prevent easy access, a small number of columns lead to a significant non-uniformity in the meridional membrane stresses.

Different support arrangements may be chosen (Figure 1.1) depending on the size of the structure [1]. For small silos, terminating columns with rings (Figure 1.1a), engaged columns (Figure 1.1b) or bracket supports (Figure 1.1e) may be suitable. On the other hand, medium and large silos require either columns extending to the eaves (Figure 1.1c) or heavy ring beams (Figure 1.1d) or double rings (Figure 1.1f).

1.2 Past Research on Buckling of Silos

Classical design treatments [2-5] assume that the meridional membrane stress in a cylindrical shell is circumferentially uniform, so that the criterion for buckling under axial compression is that corresponding to uniform compression. Recommendations given in well known design standards such as the European Standard on Strength and Stability of Shell Structures EN 1993-1-6 [6] can be used to assess the stability of a cylindrical shell under uniform compression. However, the design of a discretely supported cylindrical shell presents several challenges. Previous studies of discretely supported cylinders [7-15] have shown the great complexity of the behavior. Regardless of the arrangement, the presence of discrete supports results in meridional compressive membrane stresses that are non-uniform around the circumference, with changing patterns and decaying peak stresses with height above the supports. Each support arrangement results in a unique variation of meridional membrane stresses both in the axial and circumferential directions. Research to date on buckling above local supports has mostly focused on the locally supported cylindrical shell [14-18], which is rare in practice. By contrast, no attention has been paid to buckling of the shell in the practically important case of a shell resting on a discretely supported ring beam.

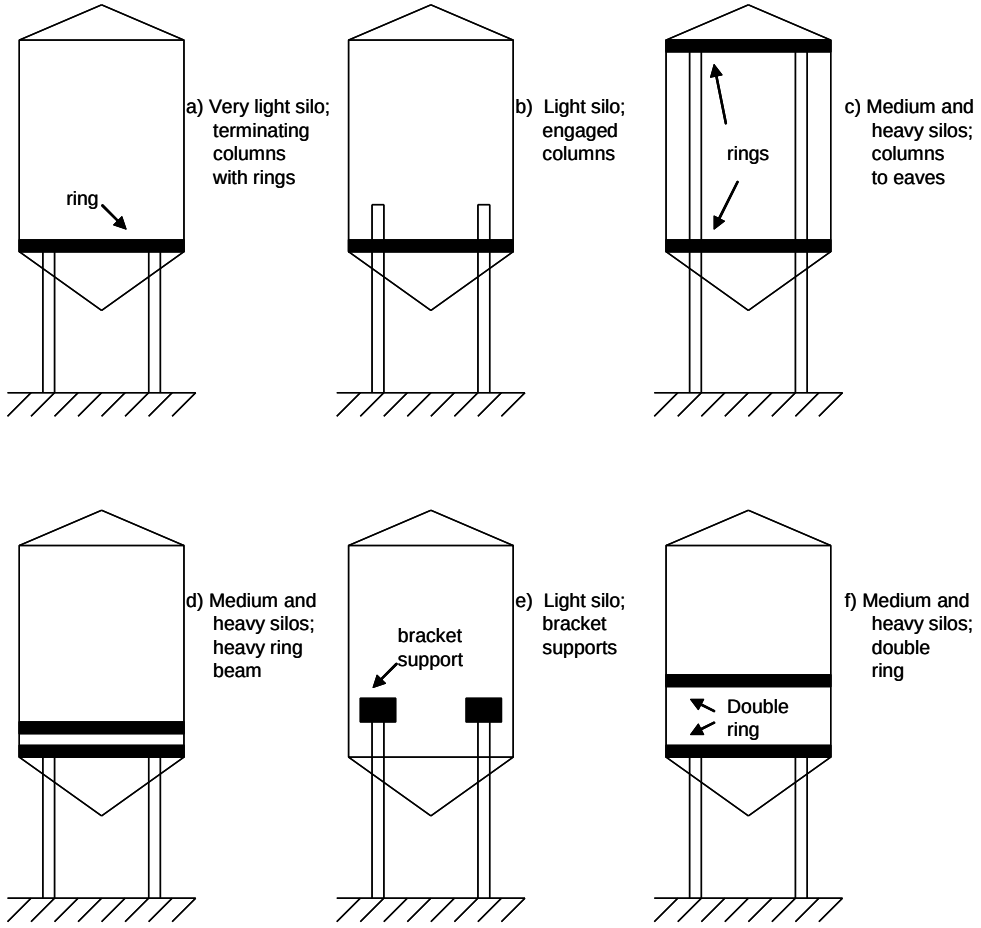

Figure 1.1: Alternative support arrangements for discretely supported silos (adapted from Rotter [1])

Topkaya and Rotter [19] studied the effect of the stiffness of a supporting ring beam for a cylindrical shell silo and devised a criterion to assess the degree of non-uniformity in meridional stresses for a given ring beam geometry. The findings of the study revealed that relatively uniform meridional stresses above the ring beam can only be achieved if very stiff ring beams are used in most applications. In most cases, non-uniformity of the meridional stresses was found to be unavoidable and must be accounted for during stability assessment of the cylindrical shell. Design standards either use the simplest traditional model outlined above, or are silent on recommending procedures for cylindrical shells resting on discrete supports.

The European Standard on Strength and Stability of Shell Structures EN 1993-1-6 [6, 20] defines the requirements for the use of numerical assessment analyses of various complexity. These are linear elastic analysis (LA), linear elastic bifurcation analysis (LBA), materially nonlinear analysis (MNA), geometrically nonlinear elastic analysis (GNA), geometrically and materially nonlinear analysis (GMNA), geometrically nonlinear elastic analysis with explicit imperfections included (GNIA), and geometrically and materially nonlinear analysis

with explicit imperfections included (GMNIA). Naturally GMNIA is the most reliable method to determine the buckling strength of any shell, but GMNIA is extremely onerous and is not suitable for routine design practice.

The LBA-MNA methodology [21] can be applied to many problems to simplify the design process. This process is based on developing a resistance curve that is based only on the reference elastic buckling and plastic resistances obtained using LBA and MNA. The design process can further be simplified if algebraic expressions can be developed for the reference resistances that the LBA and MNA analyses would produce.

1.3 Scope of the Thesis

The primary focus of this thesis is to apply the LBA-MNA methodology to shells resting on discretely supported ring beams. The problem was systematically studied through a parametric study. Finite element analyses of different complexity were conducted to obtain the buckling resistances of cylindrical shells under various assumptions. In this thesis, the details of the finite element models are given followed by the selection of design cases based on the parameters that influence the response. The results of an imperfection sensitivity study are explained. The predictions of LBA, MNA and GMNIA are presented. Finally, resistance curves are developed that can be used in design calculations in connection with known LBA and MNA reference resistances.

CHAPTER 2

FINITE ELEMENT ANALYSIS OF SHELLS RESTING ON DISCRETELY SUPPORTED RING BEAMS

2.1 Finite Element Modeling Details

Finite element analyses were conducted using the commercially available program ANSYS [22]. For a cylindrical shell resting on *n* equally spaced discrete supports, there are 2*n* planes of symmetry. A segment covering an angle of π/n as shown in Figure 2.1 was modeled to reduce the computational time. An I-shaped ring beam, details of which will be given in the following sections, was considered in this study. The cylindrical shell and the ring beam were modeled using eight-node shell elements (shell93). In all analyses, the ring beam was modeled to exhibit elastic behavior in order to prevent any kind of premature failure of this member. On the other hand, the cylindrical shell was modeled either as elastic or as elastic-plastic with kinematic hardening depending on the type of analysis conducted. For the cylindrical shell the modulus of elasticity (E) and Poisson's ratio (ν) were taken as 200 GPa and 0.3, respectively. In conducting materially nonlinear analysis different yield stress (f_y) values were considered as will be explained in the following sections. While the yield stress changes the hardening modulus was kept constant with a value equal to 2 MPa (E/100 000). This low value of hardening modulus basically reduces the effect of strain hardening to a minimum.

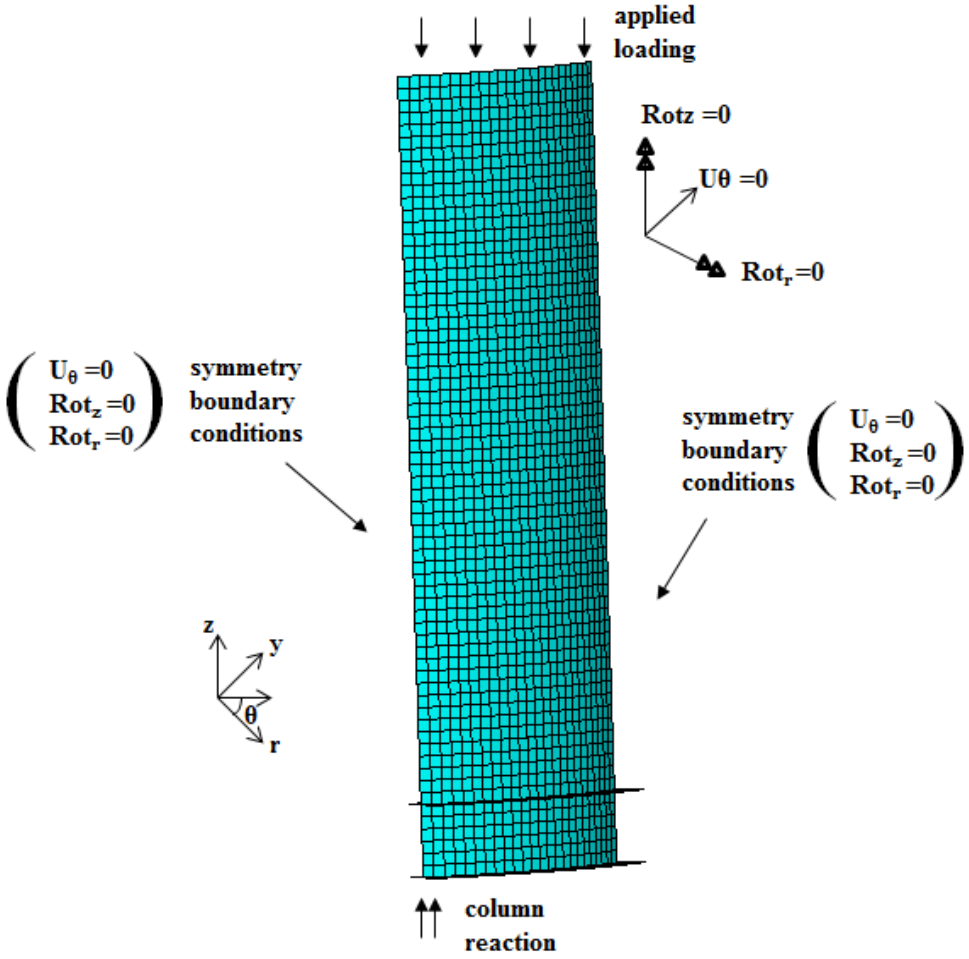

Figure 2.1: A typical finite-element mesh for the cylindrical shell and I-section ring beam

As shown in Figure 2.1, symmetry boundary conditions were applied to the nodes on each of the symmetry planes, in both the shell and the ring beam. In practice, silo cylindrical shell walls are normally connected to other conical shells at the top and the bottom, as shown in Figure 1.1. These conical shells effectively prevent out-of-round displacements of the cylindrical shell at the two extremes. The restraining effect of the connected shells was modeled by restraining the displacements at these points. At the top, both the radial and the circumferential displacements were restrained. At the bottom, the nodes shared by the cylindrical shell and the ring beam were restrained against displacement in the radial direction only. Because the ring beam is stiff in the circumferential direction, it provides a natural restraint against displacements in this direction.

Based on the study by Teng and Rotter [13], a support width-to-radius ratio of 0.2 was considered for all analysis cases. In the past, two alternatives were investigated for modeling supports. In the studies of Guggenberger [23, 24], the supports were modeled as flexible while in the studies of Rotter [13, 25] the supports were modeled as rigid. In this study the latter approach was adopted and the nodes lying within the width of the support on the base

of the ring beam were restrained against vertical movement. In the ring beam, only the nodes that coincided with the shell generators were restrained, allowing twist of the ring beam to occur at the support locations. A uniform axial load was applied to the top of the cylindrical shell around the full circumference. The magnitude of this uniform load was chosen to produce different levels of mean meridional compressive membrane stress according to the type of analysis conducted. In the nonlinear analyses, the arc-length algorithm was adopted to trace the load displacement history. Based on the mesh convergence studies, the element size was selected as 100 mm in both the axial and circumferential directions.

2.2 Linear Elastic Analysis (LA) and Selection of Analysis Cases for Parametric Study

The radius-to-thickness (r/t) ratio and the degree of non-uniformity in the meridional membrane stresses were considered as the prime variables in the parametric study. The number of supports (n) was taken as 4 throughout the study because it is the commonest number used in silo designs. The dimensions of the ring beam can be adjusted to come up with different variations of meridional membrane stresses. However, changing the ring beam dimensions, especially the web depth, introduces an additional parameter. Because the discrete support forces are transferred from the ring beam to the cylindrical shell, the depth of the ring beam has a major influence on stress pattern above it. In order to eliminate the effect of having different beam depths, it was decided to use the same beam dimensions for all cases and adjust the modulus of elasticity of the ring beam (E_{rb}). A web depth of 600 mm, a flange width of 500 mm, a web thickness of 20 mm, and a flange thickness of 25 mm were used to represent the ring beam. The modulus of elasticity of the ring beam (E_{rb}) was determined by a trial-and-error procedure for a given shell geometry and a target degree of non-uniformity.

The radius of the shell (r) was kept constant at 3000 mm in the parametric study. Shell thicknesses (t) of 3 mm, 4 mm, 6 mm, and 12 mm were adopted, resulting in radius-to-thickness ratios (r/t) of 1000, 750, 500, and 250 respectively. The fixed height of the shell (H= 6000 mm) was taken as twice the radius of the shell. The degree of non-uniformity in the meridional membrane stresses was expressed by a stress ratio (ζ). This is the ratio of the maximum meridional membrane stress above the ring beam to the applied stress at the top of the cylindrical shell (i.e. at $z = H$). Stress ratios of 1.25, 1.5, 2.0, 2.5, and 3.0 were considered which resulted in a total of twenty cases for the parametric study. Linear elastic finite element analyses (LA) were conducted for each case to obtain the value of the ring beam modulus of elasticity E_{rb} that would give the desired stress ratio. The values of E_{rb} determined for the twenty cases are reported in Table 2-1. Considering these E_{rb} values does not exactly provide the target stress ratio (ζ). The values of the target ζ and the actual ζ values are also reported in this table. Comparison of these values indicates that the maximum deviation from the target value is 0.35 percent.

Table 2-1: Cases Considered in the Parametric Study

Case Number	Radius (r) (mm)	Thickness (t) (mm)	r/t	Target ζ	Actual ζ	E_{rb} (GPa)
1	3000	3	1000	1.25	1.254	800
2	3000	3	1000	1.50	1.499	360
3	3000	3	1000	2.00	2.007	134
4	3000	3	1000	2.50	2.506	64
5	3000	3	1000	3.00	3.008	32
6	3000	4	750	1.25	1.250	1100
7	3000	4	750	1.50	1.500	488
8	3000	4	750	2.00	2.005	184
9	3000	4	750	2.50	2.502	89
10	3000	4	750	3.00	3.004	45
11	3000	6	500	1.25	1.249	1700
12	3000	6	500	1.50	1.497	760
13	3000	6	500	2.00	2.002	290
14	3000	6	500	2.50	2.502	142
15	3000	6	500	3.00	2.994	74
16	3000	12	250	1.25	1.250	3600
17	3000	12	250	1.50	1.504	1600
18	3000	12	250	2.00	2.006	630
19	3000	12	250	2.50	2.501	318
20	3000	12	250	3.00	3.001	168

Circumferential variation of meridional membrane stress above ring beam is given in Figure 2.2 for the r/t ratios considered in this study. In general, variations for a particular stress ratio (ζ) is very similar for different r/t ratios. This enables direct comparison of results for a particular stress ratio (ζ) with different r/t ratios.

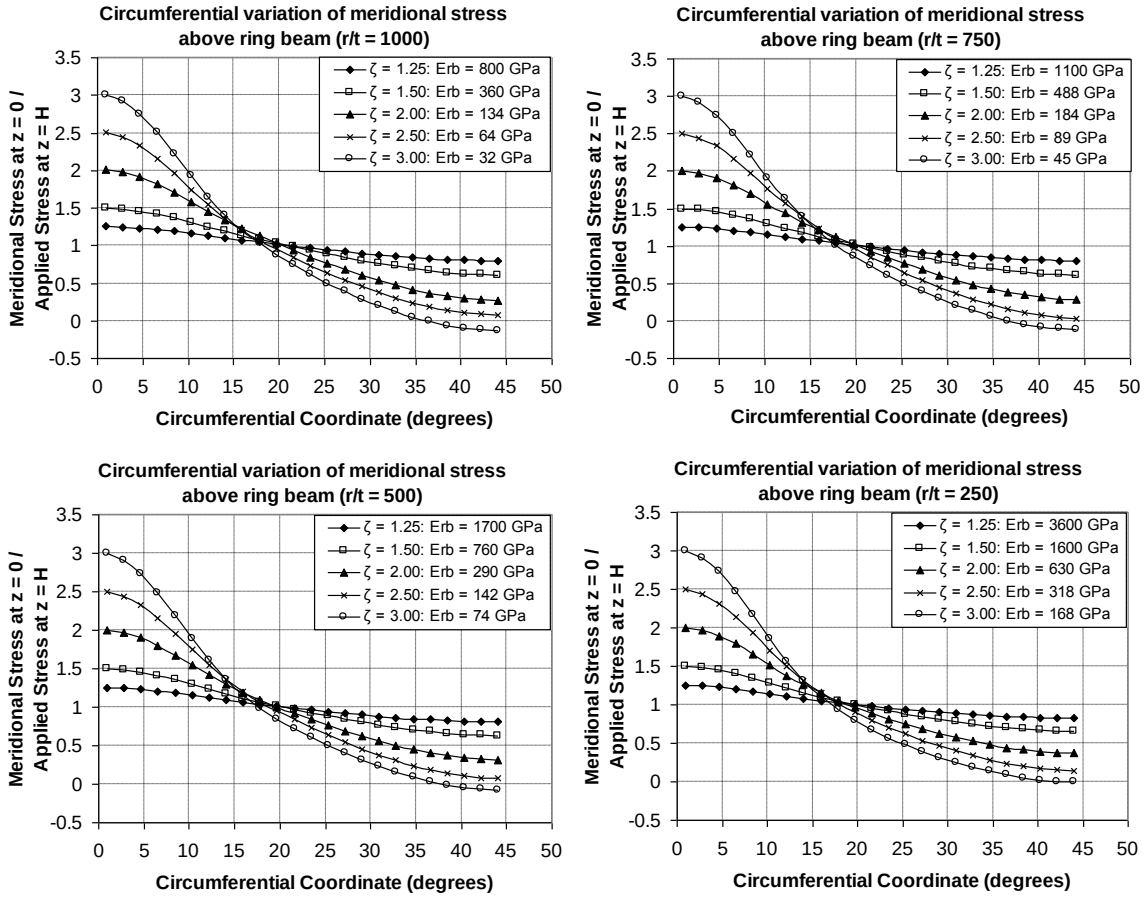

Figure 2.2: Circumferential variation of meridional stress above ring beam for various *r*/*t* ratios

2.3 Linear Elastic Bifurcation Analysis (LBA)

Due to the imperfection sensitivity of shell structures and potential inelastic behavior, the elastic buckling loads obtained from a bifurcation analysis are far from the actual failure loads. However, the elastic critical buckling load is still used because it provides a reference. For a cylindrical shell under uniform compression the classical elastic stress (σ_{cl}) that causes instability [26-28] can be expressed as follows:

$$\sigma_{cl} = \frac{E}{\sqrt{3\left(1-\nu^2\right)}}\frac{t}{r} \approx 0.605E\frac{t}{r} \qquad (1)$$

Libai and Durban [29] studied the linear bifurcation buckling (LBA) of cylindrical shells subjected to a cosinusoidally varying edge axial load and found that the elastic critical stress under non-uniform loading was slightly higher than that for uniform loading. They defined a loading parameter (k_p) as:

$$k_p = \frac{n}{\left[12(1-\nu^2)\right]^{1/4}}\sqrt{\frac{t}{r}} = n\sqrt{\frac{\sigma_{cl}}{2E}} \tag{2}$$

Three regions were identified and for the small k_p region $\left(0 \le k_p \le 0.39\right)$ the following relationship was proposed based on curve-fit to numerical analysis data.

$$\sigma_{cosine} = \sigma_{cl}\left[1 + \frac{5}{6}k_p^{\sqrt{2}}\right] \tag{3}$$

where σ_{cosine} is the linear elastic bifurcation stress (LBA) under cosine loading.

For the 20 cases considered in this study the term in the square brackets in Equation 3 has a maximum value of 1.05 for cases with r/t=250. In practice this means that the critical stress under uniform compression is identical to the peak critical membrane stress under cosine loading [30]. This may alternatively be stated as the shell buckles when the maximum value of the non-uniform axial membrane compressive stress reaches to the classical elastic stress given in Equation 1.

A set of linear elastic bifurcation analysis was conducted to obtain elastic buckling loads for cylinders that rest on discretely supported ring beams. All 20 cases were analyzed. The cylinders were subjected to uniform compressive stresses at the top boundary. The uniform stress that causes buckling were obtained and are given in normalized form in Figure 2.3. In this figure the results for the 20 cases are presented. The stress that causes buckling which is termed as σ_{LBA} is normalized by the classical elastic buckling stress divided by the stress ratio (σ_{cl}/ζ). The values presented in Figure 2.3 indicate that the elastic buckling stresses from an eigenvalue analysis (LBA) are slightly greater than the stresses obtained by dividing the classical elastic buckling stress by the stress ratio. It should be noted that the circumferential variation of meridional stresses above the ring beam (Figure 2.2) cannot be directly represented by a pure cosine loading. The variation of meridional stresses resemble cosine loading as the degree of non-uniformity is more pronounced. Nonetheless, it is observed that the increase in buckling resistance is far more than the increase expected according to Equation 3.

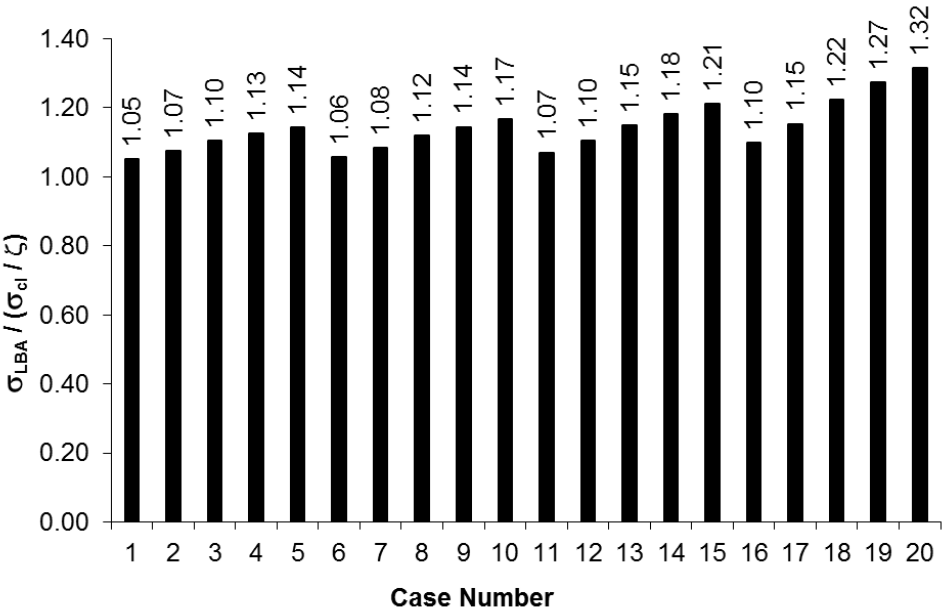

Figure 2.3: The difference between the peak stress at the critical (LBA) bifurcation load and the classical elastic critical stress for uniform compression

A curve-fitting procedure was applied to the data to effectively represent the linear elastic buckling stresses (σ_{LBA}). The results presented in Figure 2.3 reveal that the ratios depend on r/t ratio and stress ratio (ζ). The following expression which is particular to 4 column supports can be used to estimate the buckling stress of a cylindrical shell resting on discretely supported ring beams.

$$\sigma_{LBA} = \frac{\sigma_{cl}}{\zeta}\left[1 + C_1(\zeta - 1)^{C_2}\right] \qquad (4)$$

$$\textit{where} \quad C_1 = 4.6\left(\frac{r}{t}\right)^{-0.55} \qquad C_2 = 0.9\left(\frac{r}{t}\right)^{-0.08}$$

A comparison of the numerical analysis results and quality of estimations offered by Equation 4 is given in Figure 2.4. As demonstrated in this figure, the proposed capacity equation is capable of representing the numerical findings. It should be emphasized that omitting the square bracket term in Equation 4 provides conservative estimates and finding elastic buckling stresses from classical elastic buckling stress divided by the stress ratio is a safe approach.

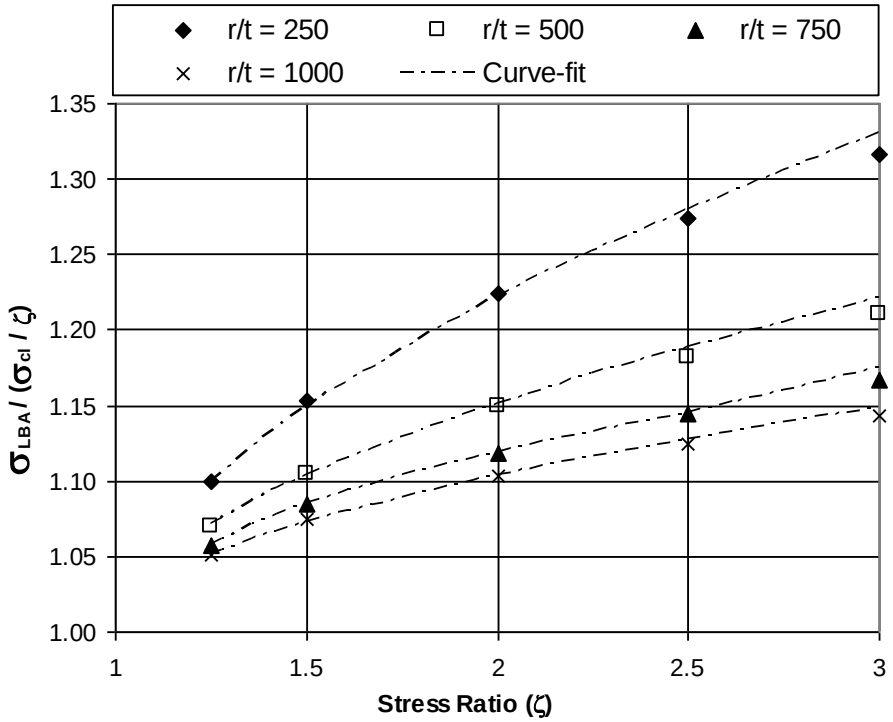

Figure 2.4: Illustration of the accuracy of Equation 4

2.4 Elastic Imperfection Sensitivity Study – GNA and GNIA

As explained in the previous section, linear elastic bifurcation analysis results have a little meaning because shells are sensitive to imperfections. A systematic study has been undertaken to study the imperfection sensitivity of cylindrical shells resting on discretely supported ring beams. The form of imperfection and its amplitude are the two utmost important parameters that should be taken into account in the imperfection sensitivity study. In general it would be suitable to directly adopt a measured pattern of imperfection form. Unfortunately, the form of imperfections on ring supported shells, especially above the support locations has not been explored in the past. The European design recommendations for Strength and Stability of Shell Structures EN 1993-1-6 [6] recommends the eigenmode-affine pattern should be used in analysis unless a different unfavorable pattern can be justified. The recommendations given in EN 1993-1-6 [6] was adopted in this study and the eigenmode-affine imperfection pattern was used throughout.

Representative linear eigenmode shapes for various stress ratios and an *r*/*t* ratio of 1000 are given in Figure 2.5. These shapes are extracted using a linear elastic bifurcation analysis. The radial displacement pattern for the meridian right above the support ($\theta = 0$) is given in Figure 2.5. According to this figure the imperfections are more confined to the support location as the stress ratio increases. While the imperfections decay at about 2300 mm for a stress ratio of 1.25, decay in imperfections is observed at about 1300 mm for a stress ratio of 3.00. The other observation is related to the direction of waves among different stress ratios. The first half-wave is oriented inwards for all cases except for the stress ratio of 1.50, where

the half-wave is oriented outwards. All eigenmodes are output by the computational module such that the maximum value of the shape reaches to unity as shown in Figure 2.5.

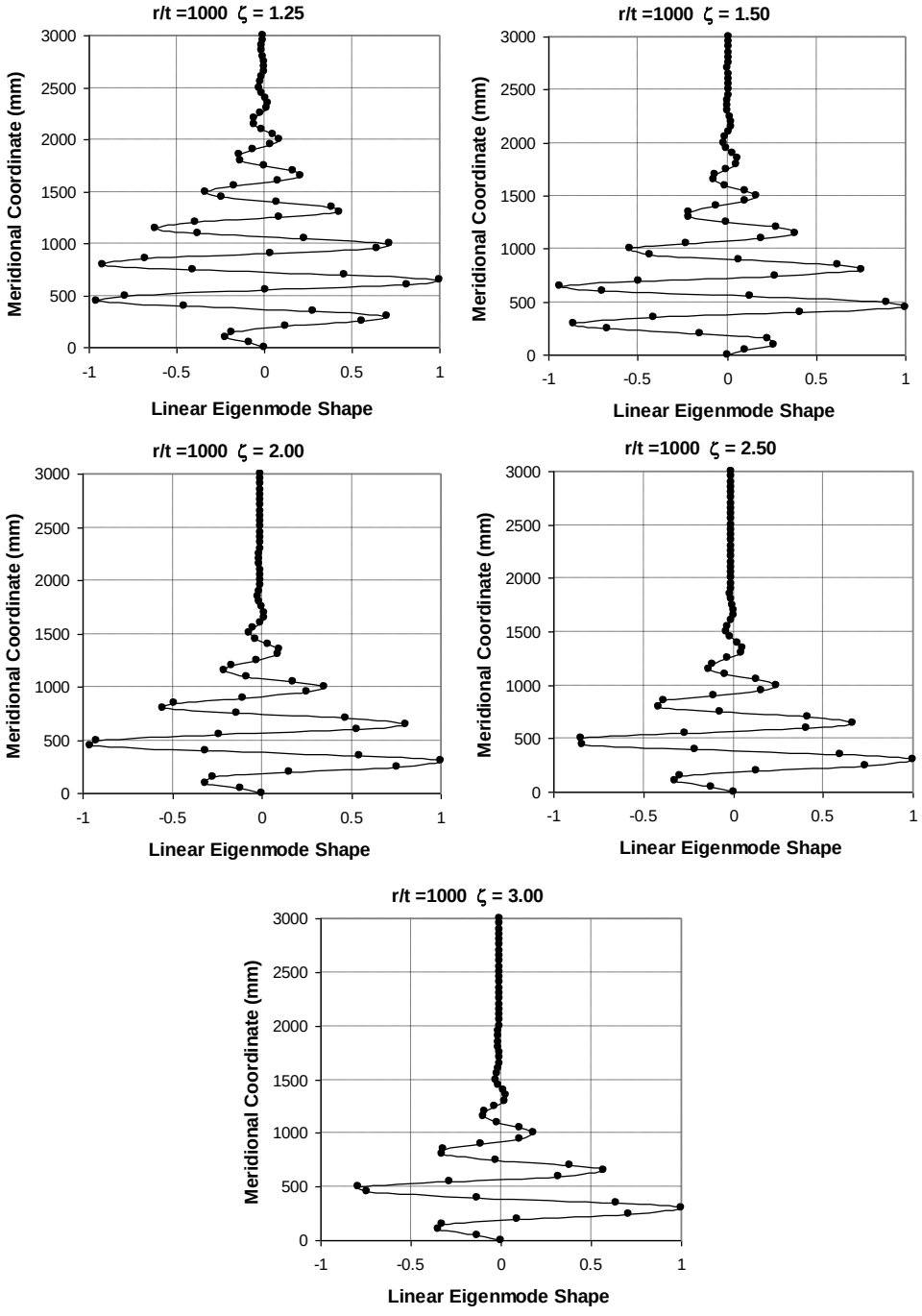

Figure 2.5: Typical linear eigenmodes (LBA) for r/t = 1000

Imperfections as well as geometrical effects influence the buckling capacity of shells. In order to distinguish the effects of these, geometrically nonlinear analyses (GNA) were conducted on the selected analysis cases first. The path follower algorithm was adopted to trace the load displacement history. In general, applying loads until a target displacement is a computationally demanding procedure. Because the interest is a limit load in this study, another failure criterion which significantly reduces the analysis time was incorporated. In this procedure the analysis is terminated once the tangent stiffness matrix becomes singular. This indicates that a limit load is reached. A representative applied stress versus axial displacement of the meridian at $\theta = 0$ is given in Figure 2.6. Behavior for $r/t = 250$ and $\zeta = 3.00$ (Case 20) is presented. Two different procedures for terminating the analysis routine are given. In the first one the analysis is continued until behavior goes into the post buckling regime. In the other one the analysis is terminated when the tangent stiffness matrix becomes singular and the analysis is cut short at the load step shown with a circle on the applied stress versus axial shortening graph.

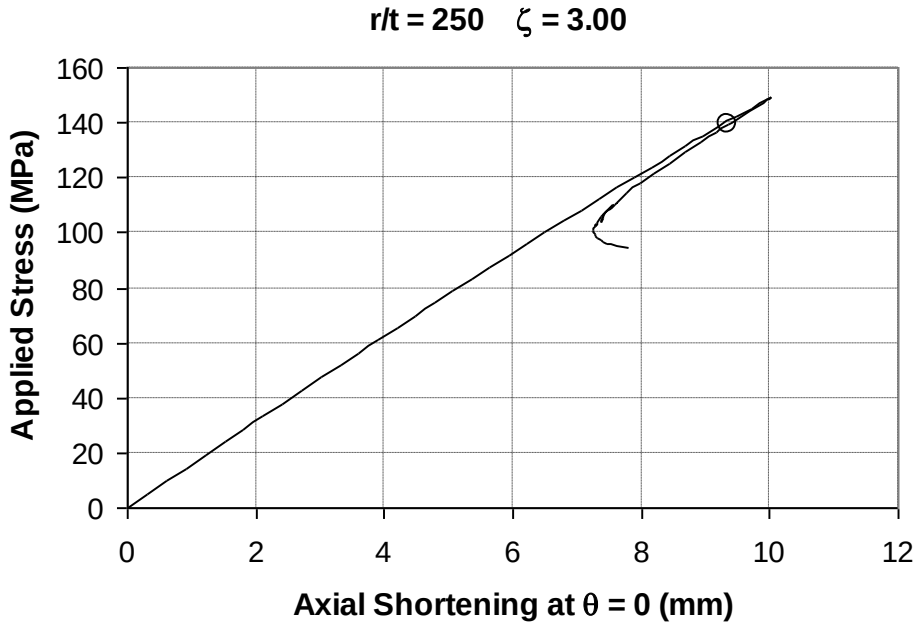

Figure 2.6: Typical load-displacement curve for an elastic locally support cylinder

By adopting the computational procedure explained above the GNA resistances were obtained. The results of the GNA analysis are presented in Figure 2.7, where the resistance from GNA (σ_{GNA}) is normalized with the resistance obtained using linear elastic bifurcation analysis (LBA) (σ_{LBA}). The analysis results indicate that the geometrical effects are more pronounced as the r/t ratio decreases and the stress ratio increases. In general, the decrease in buckling stresses is between 4 to 33 percent due to geometrical effects.

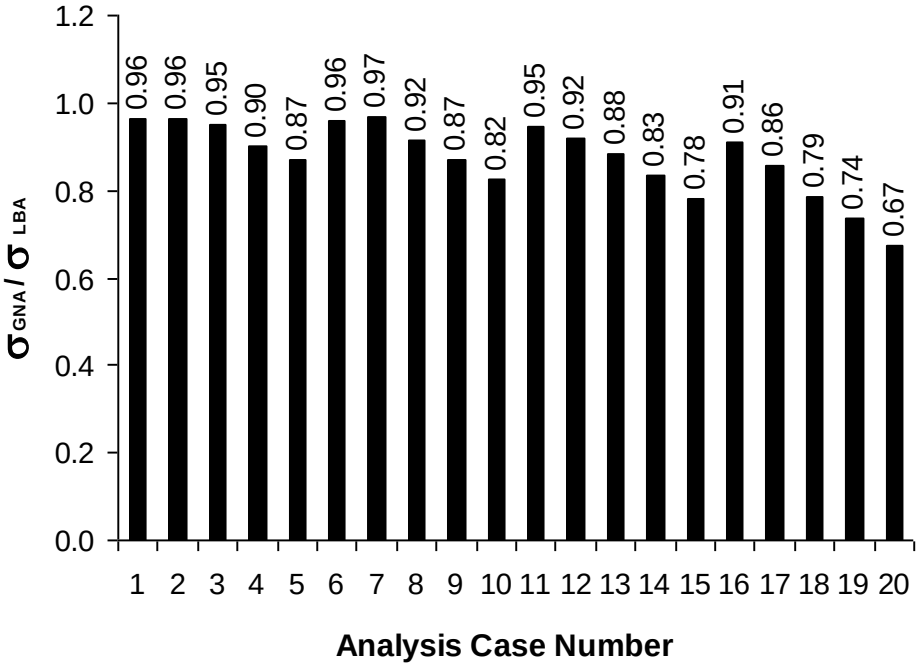

Figure 2.7: The effect of geometric nonlinearity: Nonlinear elastic buckling strength relative to the critical load (GNA/LBA)

In order to study the effect of imperfections a set of geometrically nonlinear elastic analysis with imperfections included (GNIA) was conducted. In this study the effects of having different imperfection amplitudes were also explored. According to EN 1993-1-6 [6] the sign of equivalent geometric imperfections should be chosen in such a manner that the maximum initial shape deviations are unfavorably oriented towards the center of the shell curvature. This means that the imperfection shapes given in Figure 2.5 should be reversed such that the maximum initial shape deviation is pointing inwards rather than outwards. However, in the preliminary stages of the study it was discovered that most unfavorable is not always represented by imperfections that point inwards. Due to the complexity of the imperfection shapes shown in Figure 2.5 and the complexity of loading, the outward pointing imperfections can give lower buckling stresses when compared with inward pointing imperfections. To take this behavior into account, two analyses were conducted for each case; one with inward and the other with outward imperfections. The minimum of two resistances are reported herein for the GNIA results.

Dimensionless imperfection amplitudes (Δ_o/t) of 0.1, 0.2, 0.5, 1.0, 2.0, 3.0 were considered. A total of 240 GNIA were conducted. The results are presented in Figures 2.8 and 2.9 in normalized form. In Figure 2.8, the GNIA resistances are normalized by the GNA resistances and in Figure 2.9, the GNIA resistances are normalized by the LBA resistances. The ratio of GNIA/GNA is an indication of the imperfection effects on the buckling stresses without the geometrical effects. The ratio of GNIA/LBA is an indication of the combined

geometrical and imperfection effects on the buckling resistance. In general, the GNIA/LBA ratio provides the knock down factor (α) and the GNIA/GNA ratio provides the imperfection component of the knock down factor (α_I). The results presented in Figure 2.8 indicate that the GNIA/GNA ratios fall within a large band between 0.5 and 0.9. In general, the ratios increase as the r/t value decreases. This is exactly the opposite of what is observed for the GNA/LBA ratio. The results presented in Figure 2.9 indicate that the GNIA/LBA results fall within a narrow band between 0.5 and 0.7. No definite conclusions can be drawn related with the imperfection amplitude. In general, the buckling resistance decreases as Δ_o/t increases to 0.2 from 0.1. The resistances tend to increase as Δ_o/t increases to 0.5 from 0.2. The resistances show a decreasing trend for Δ_o/t ratios that are greater than 0.5. Similar observations were reported by Guggenberger et al. [14] where shells having higher imperfection amplitudes exhibit slightly greater strength compared to shells with smaller imperfection amplitudes. Data presented in Figure 2.9 indicate that a conservative lower bound value of 0.5 can be adopted for the knock down factor (α).

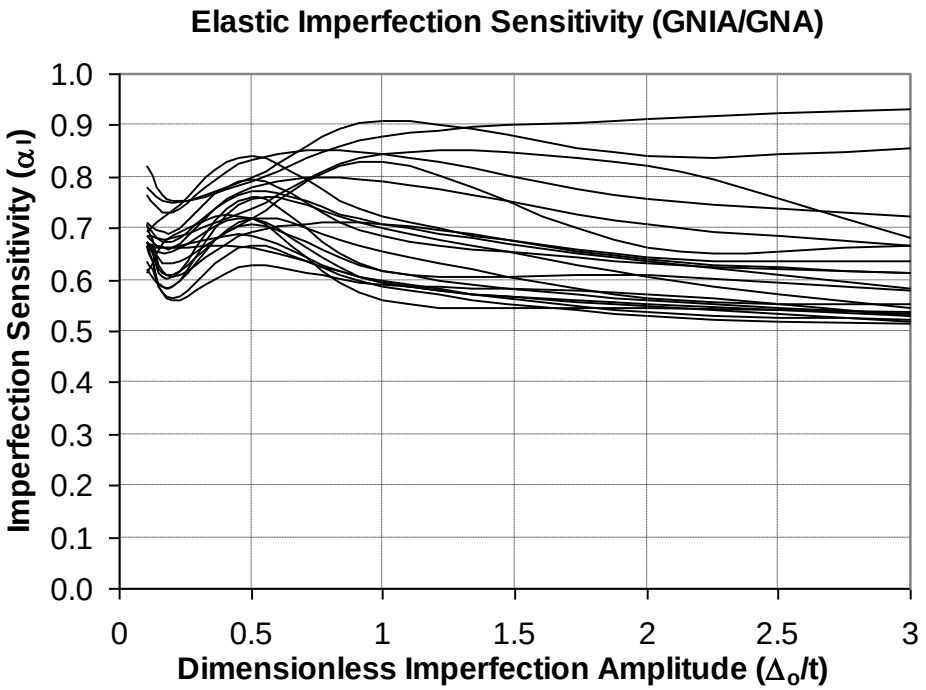

Figure 2.8: Elastic imperfection sensitivity curves relative to nonlinear elastic buckling load (GNIA/GNA)

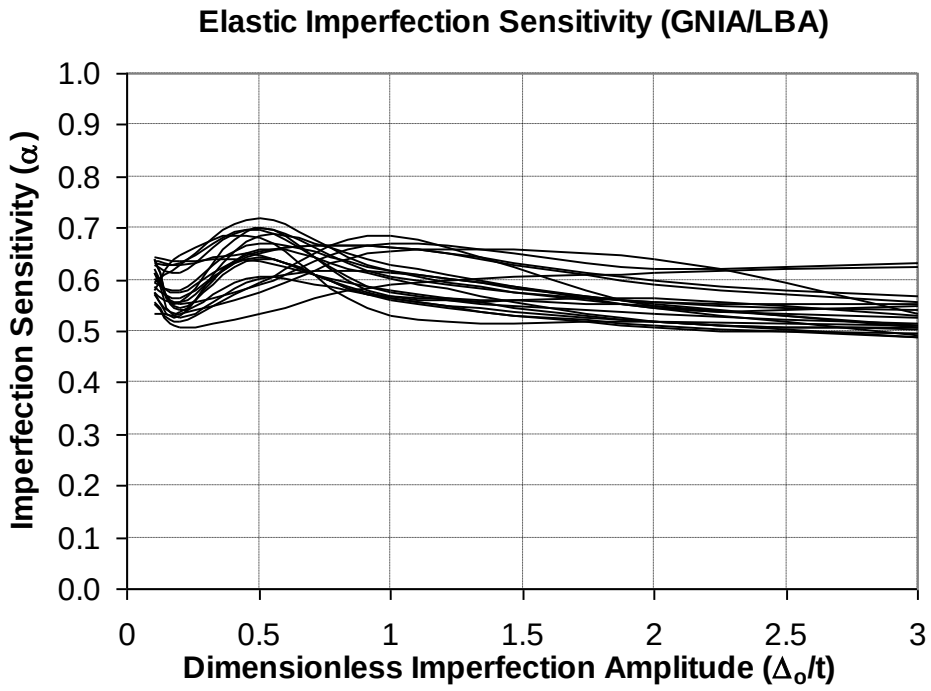

Figure 2.9: Elastic imperfection sensitivity curves relative to critical load (GNIA/LBA)

2.5 Materially Nonlinear Analysis (MNA)

The plastic collapse load can be determined from a materially nonlinear analysis (MNA). In general, it is expected that the entire cross section of the cylindrical shell to yield in the case of uniform applied compression. When the cylindrical shell rests on a discretely supported ring beam, yielding is expected to initiate at lower levels of applied load due to the non-uniformity of meridional stress above the ring beam. In order to determine plastic collapse loads a set of MNA was conducted. The preliminary analysis results indicate that the behavior is not dependent on the level of yield stress. Representative load deformation relationships for various stress ratios are given in Figure 2.10, for $r/t = 1000$. Similar results were obtained for other r/t ratios. Cases with high stress ratios result in earlier yielding and loss of stiffness, eventually the applied stress over the yield stress value reaches to unity. This means that all fibers in the meridional direction reach to their yield stress regardless of the stress ratio.

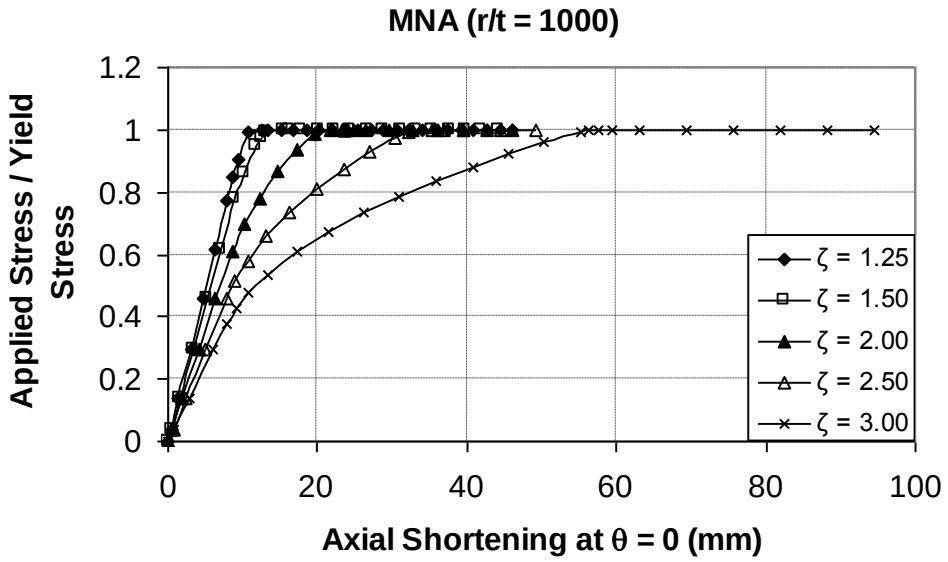

Figure 2.10: Materially nonlinear analysis load-deformation curves for *r/t* = 1000

The ring beam is responsible for redistribution of meridional stresses. Once the fibers above the support location yields, the stresses are redistributed due to the ductile nature of structural steel. A plot of von Mises plastic strains at plastic collapse are given in Figure 2.11 for *r*/*t* = 1000 and a stress ratio of 3.0. As shown in this figure, majority of the fibers close to the support location experience high plastic strains. The plastic resistance is reached when all fibers at the top reach to the yield stress.

Based on the finite element analysis results, the applied stress which causes plastic resistance to develop (σ_{MNA}) can be expressed as follows:

$$\sigma_{MNA} = f_y \tag{5}$$

where f_y is the yield stress of steel.

Equation 5 can be directly used in MNA-LBA methodology which will be developed in the following sections of this thesis for the particular problem of interest.

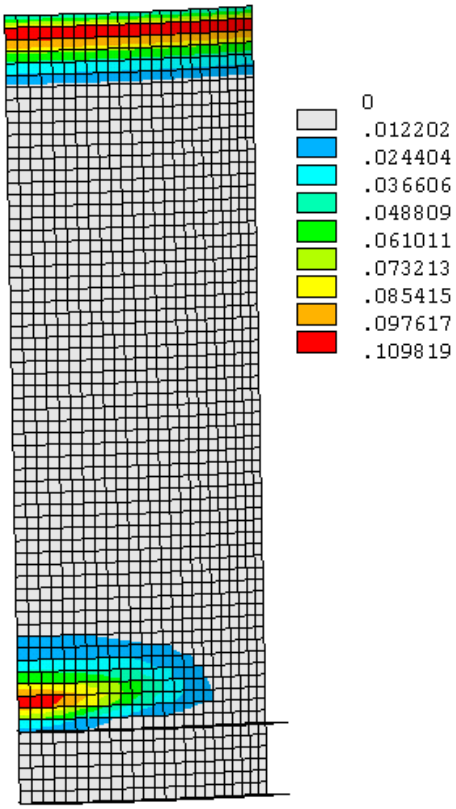

Figure 2.11: von Mises plastic strains for materially nonlinear analysis: $\zeta = 3.00$; $r/t = 1000$

2.6 The MNA-LBA Methodology

The generalized resistance curve shown in Figure 2.12 is used in design of many structural members [31]. In general, the characteristic resistance of a member or a system is defined as follows:

$$R_k = \chi R_{pl} \qquad \sigma_{\mathrm{GMNIA}} = \chi \sigma_{MNA} \tag{6}$$

where R_k is the characteristic resistance, R_{pl} is the plastic resistance, χ is the reduction factor, which is the ratio of the characteristic resistance to plastic resistance. For the cylindrical shell resting on a discretely supported ring beam, the characteristic resistance and plastic resistance are identical to the resistance obtained using an analysis which includes material and geometric nonlinearities with imperfections (σ_{GMNIA}) and to the resistance obtained using a materially nonlinear analysis (σ_{MNA}), respectively.

In order to represent the resistance curve in an effective manner two key reference resistances are required. The first one is the elastic critical resistance (R_{cr}) defined as the lowest eigenvalue in a linear bifurcation analysis. For the particular problem of interest, the critical elastic resistance corresponds to the resistance obtained using a linear elastic bifurcation analysis (σ_{LBA}). The second reference resistance is the plastic resistance (R_{pl})

which is defined as the lowest collapse load arising from small displacement theory rigid plastic calculation. Based on these two reference resistances the non-dimensional slenderness can be expressed as follows:

$$\bar{\lambda} = \sqrt{\frac{R_{pl}}{R_{cr}}} = \sqrt{\frac{\sigma_{MNA}}{\sigma_{LBA}}} \tag{7}$$

Based on non-dimensional slenderness, the behavior is usually divided into three regimes as shown in Figure 2.12. The first regime corresponds to a plastic plateau or a hardening zone, if it exists, for non-dimensional slenderness values less than a squash limit relative slenderness termed as $\bar{\lambda}_o$. The second regime corresponds to elastic-plastic interaction and is for non-dimensional slenderness values between $\bar{\lambda}_o$ and threshold slenderness which distinguishes between elastic and inelastic buckling, $\bar{\lambda}_p$. The third regime corresponds to elastic buckling and is valid for non-dimensional slenderness values greater than $\bar{\lambda}_p$.

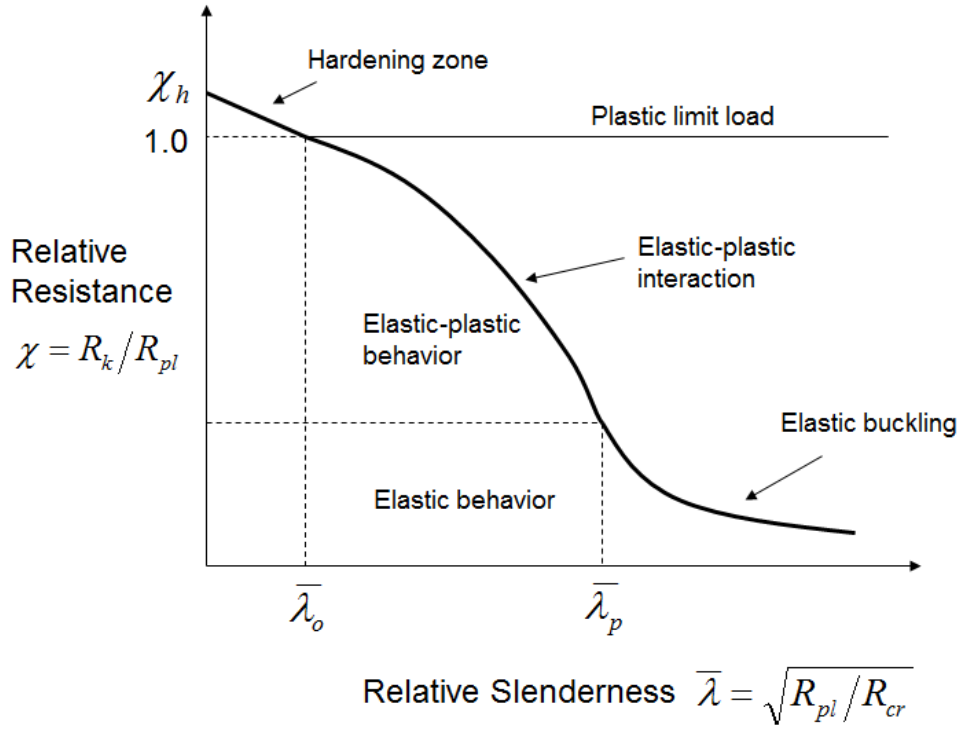

Figure 2.12: The generalized capacity curve for structural systems (adapted from Rotter[31])

The reduction factor (χ) which defines the resistance curve can be expressed as follows:

$$\chi = \chi_h - \left(\frac{\bar{\bar{\lambda}}}{\bar{\bar{\lambda}}_o}\right)(\chi_h - 1) \quad \text{when} \quad \bar{\bar{\lambda}} \le \bar{\bar{\lambda}}_o \tag{8}$$

$$\chi = 1 - \beta\left(\frac{\bar{\bar{\lambda}} - \bar{\bar{\lambda}}_o}{\bar{\bar{\lambda}}_p - \bar{\bar{\lambda}}_o}\right)^{\eta} \quad \text{when} \quad \bar{\bar{\lambda}}_o < \bar{\bar{\lambda}} < \bar{\bar{\lambda}}_p \tag{9}$$

$$\chi = \frac{\alpha}{\bar{\bar{\lambda}}^2} \quad \text{when} \quad \bar{\bar{\lambda}}_p \le \bar{\bar{\lambda}} \tag{10}$$

in which α is the elastic imperfection and nonlinearity factor (knock down factor), β is the plastic range factor, η is the interaction exponent, and $\bar{\bar{\lambda}}_p$ is defined as:

$$\bar{\bar{\lambda}}_p = \sqrt{\frac{\alpha}{1-\beta}} \tag{11}$$

The procedure for finding parameters of the resistance curve from computer calculations is explained by Rotter [31]. This procedure requires calculating characteristic resistances (σ_{GMNIA}) for a constant dimensionless imperfection amplitude and constant geometric non-linearity. The results from GMNIA analysis are then plotted as shown in Figure 2.13 to extract the parameters. By making use of a plot shown in Figure 2.13 the parameters α, β, *k*, χ_h can be found easily. Once these parameters are found the value of η can be found as follows:

$$\eta = \frac{\ln(1-k) - \ln(\beta)}{\ln(\sqrt{\alpha} - \bar{\bar{\lambda}}_o) - \ln(\sqrt{\alpha/1-\beta} - \bar{\bar{\lambda}}_o)} \tag{12}$$

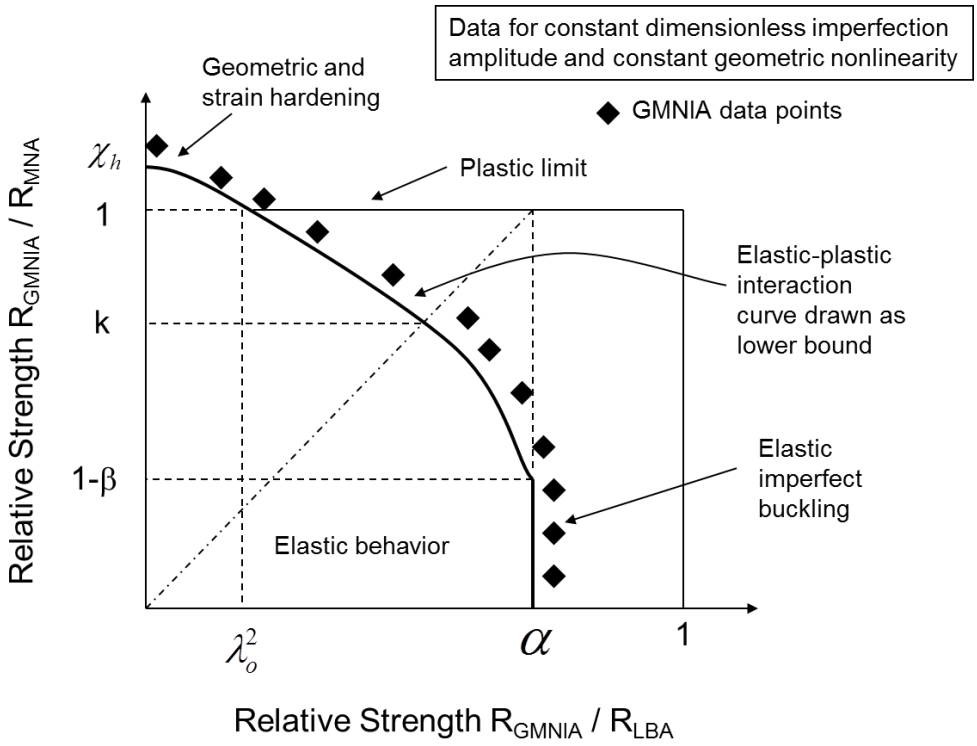

Figure 2.13: Plot for formal extraction of the capacity curve parameters (adapted from Rotter[31])

2.7 Geometrically and Materially Nonlinear Analysis with and without Imperfections (GMNA and GMNIA) and Development of Resistance Curves

Finally, geometrically and materially nonlinear analyses with imperfections (GMNIA) were conducted to characterize the strength possessed by cylindrical shells resting on discretely supported ring beams. Additional analyses based on geometrical and material nonlinearities without imperfections (GMNA) were also completed to observe the influence of imperfections on the characteristic strength. As mentioned before, data given in Figure 2.13 has to be produced such that the geometric imperfection amplitude and geometrically nonlinear effects affect all the results to the same extent. This can be accomplished by retaining the same dimensionless geometry and modulus, but changing the yield stress. The 20 cases given in Table 2.1 were considered and the yield stress (f_y) value was considered to be equal to 1 MPa, 10, MPa, 25 MPa, 50 MPa, 75 MPa, 100 MPa, 150 MPa, 200 MPa, 300 MPa, and 600 MPa, resulting in 200 analysis cases. For the GMNIA analysis two different imperfection amplitudes were considered. These were Δ_o/t = 0.2, and Δ_o/t = 3.0. The selected imperfection amplitudes covers a wide range and as demonstrated through GNIA analyses the differences between these two imperfection amplitudes are expected to be less. The eigenmode-affine pattern was

used for imperfections and both inward and outward imperfections were considered which resulted in a total of 800 GMNIA. Similarly, 200 GMNA were conducted without considering imperfections but changing the geometry and yield stress.

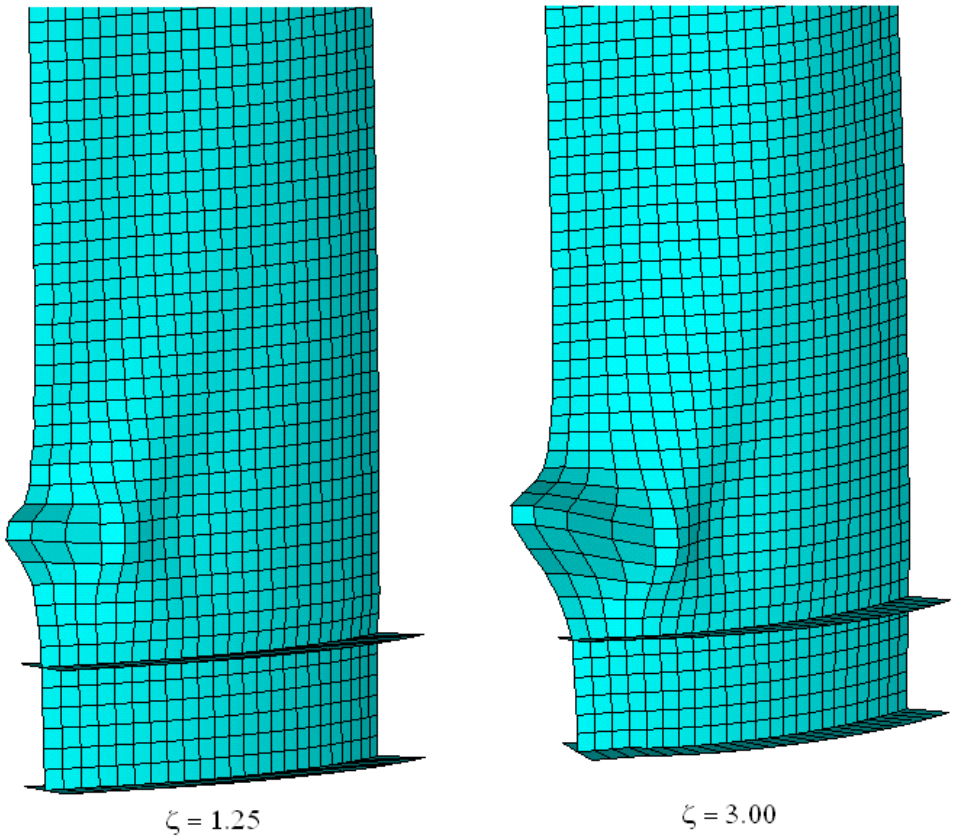

Figure 2.14: Representative buckle forms for r/t = 1000 from GMNIA (Magnification = 50 times)

Representative buckled shapes from GMNIA are given in Figure 2.14 for r/t =1000 and ζ = 1.25 and ζ = 3.00. In general, the buckle forms above the support point having a half sine wave where the peak is towards the center of shell curvature. The results from GMNA and GMNIA are compared in Figure 2.15. In this figure the reduction factor values are plotted against the non-dimensional slenderness. The results for Δ_o/t = 0.2 is used for GMNIA and the worst result from either of the inward or outward imperfection pattern is considered. The perfectly elastic behavior $\chi = 1/\bar{\lambda}^2$ is also plotted in this figure for comparison. For large values of non-dimensionless slenderness, the GMNA results generally fall on the curve for perfectly elastic behavior while some data points are below the curve. This is due to the geometrical effects as explored in the previous sections. The GMNIA results in lower reduction factors as compared to GMNA for this region. For low values of non-dimensionless slenderness the GMNIA and GMNA results are similar for some cases indicating the imperfections have a small contribution to resistance while some large differences are observed for other cases.

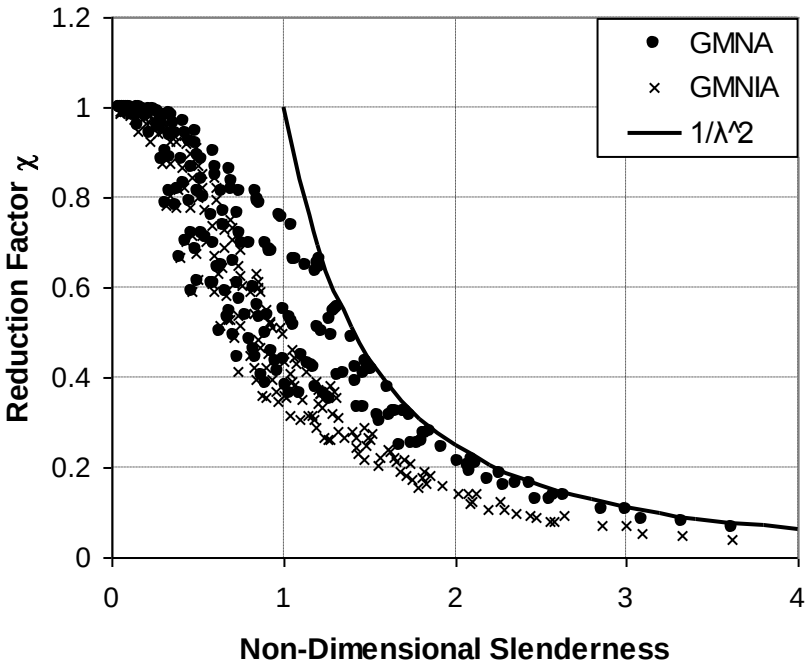

Figure 2.15: Comparison of perfect and imperfect shell buckling strengths (GMNA and GMNIA)

In order to develop the parameters for the resistance curves the results are plotted in non-dimensional form as demonstrated in Figure 2.13. The data is plotted in Figures 2.16 and 2.17 for $\Delta_o/t = 0.2$, and $\Delta_o/t = 3.0$, respectively. It is worthwhile to note that the differences between the two imperfection amplitudes are generally small. For the 200 analysis cases the ratio of resistances obtained using $\Delta_o/t = 3.0$ to $\Delta_o/t = 0.2$ has an average, standard deviation, maximum, and minimum of 0.93, 0.09, 1.24, 0.78, respectively. These values indicate that the $\Delta_o/t = 3.0$ case produces capacities that are on average 7 percent lower than the capacities produced using $\Delta_o/t = 0.2$. The maximum deviations are on the order of 25 percent. It can be concluded that either of the imperfection amplitudes can be used to develop resistance curves because the effect of imperfections between the two imperfection amplitudes are on negligible order.

The data presented in Figures 2.16 and 2.17 reveal that the parameters for the resistance curves do not have to depend on the r/t ratio. Trends for various r/t ratios are similar with minor differences. Based on these observations the parameters for the resistance curves were determined considering the data for $\Delta_o/t = 0.2$. The parameters are outlined in Table 2-2. It is worthwhile to note that the knock down factor is 0.5 regardless of the stress ratio (ζ) as demonstrated earlier in the section on GNIA. The stress ratio (ζ) has a profound effect on the β value. The β values tend to increase as the ζ value increases. This is natural, because the stress concentration which is more pronounced for high stress ratios result in early yielding of the cylindrical shell. In all cases no hardening behavior is observed due

to the assumed low hardening modulus for steel. This resulted in a $\overline{\lambda}_o$ value which is equal to zero for all cases, eliminating the first region of the interaction curve completely. The intercept factor (k) is inversely proportional to the stress ratio which eventually resulted in η values that vary inversely with the stress ratio too.

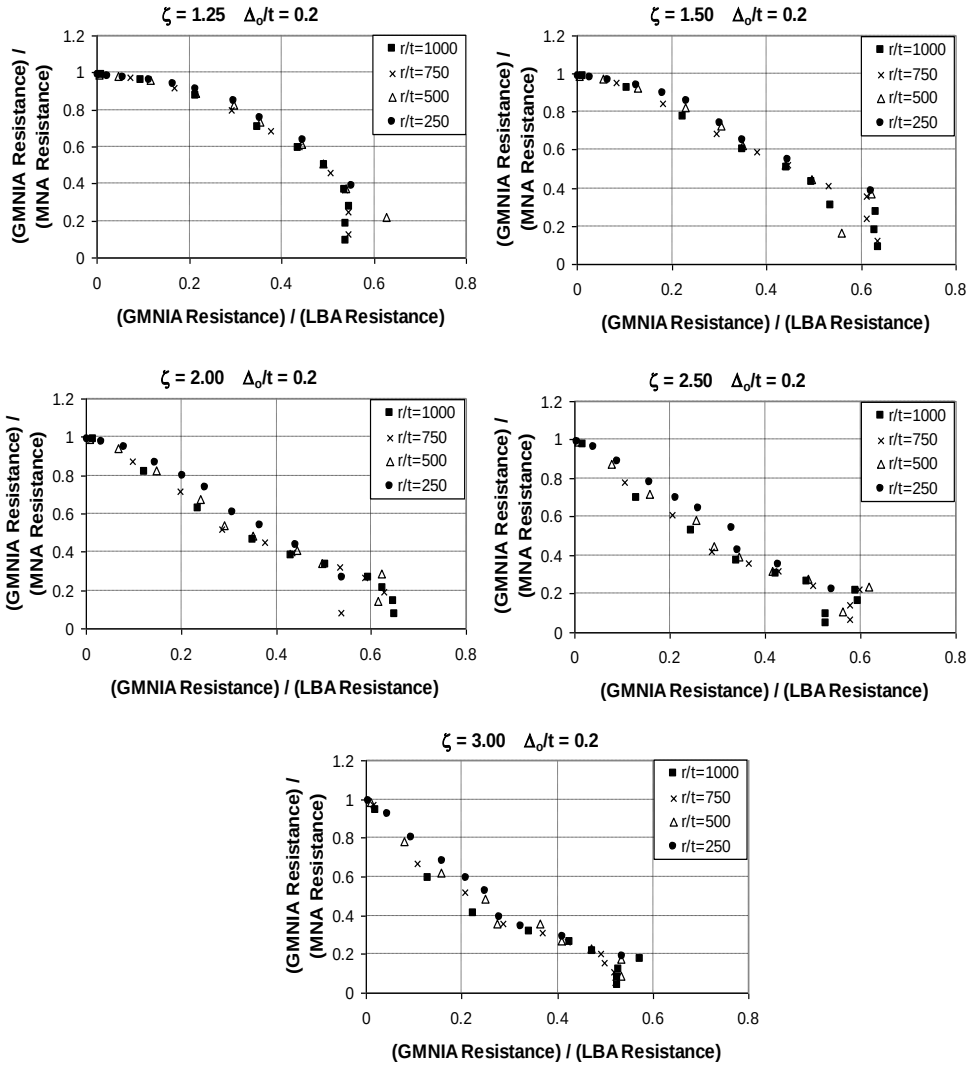

Figure 2.16: GMNIA buckling strength predictions for $\Delta_o/t = 0.2$

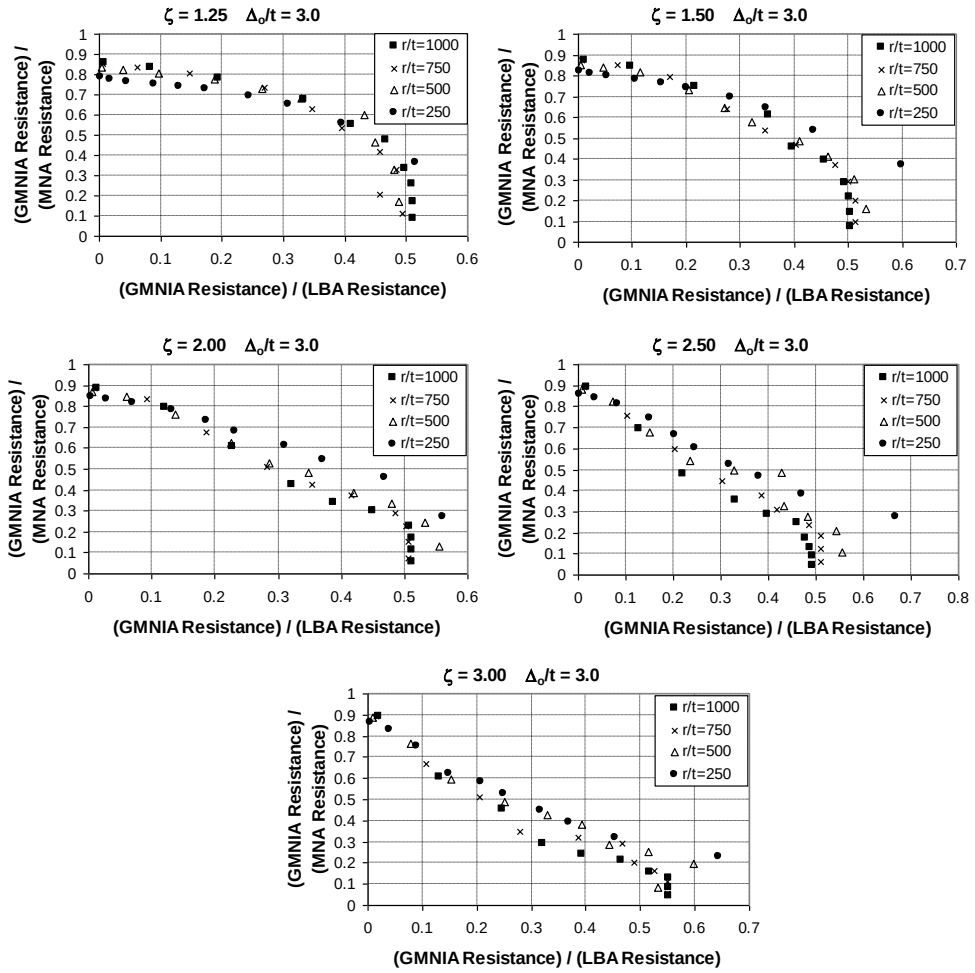

Figure 2.17: GMNIA buckling strength predictions for $\Delta_o/t = 3.0$

Table 2-2: Resistance Curve Parameters

	ζ				
	1.25	**1.5**	**2**	**2.5**	**3**
α	0.5	0.5	0.5	0.5	0.5
β	0.5	0.6	0.65	0.8	0.85
$\bar{\bar{\lambda}}_0$	0	0	0	0	0
k	0.7	0.65	0.6	0.5	0.5
η	1.47	1.18	0.92	0.58	0.56
$\bar{\bar{\lambda}}_p$	1.00	1.12	1.20	1.58	1.83

Comparison of the characteristic resistances obtained using GMNIA and the proposed resistance curves are given in Figure 2.18. The comparisons indicate that the proposed curves are capable of accurately representing the behavior. Some degree of unconservatism is present for $\Delta_o/t = 3.0$ for low value of non-dimensional slenderness. The unconservative estimates are not considered detrimental because the shells in this region are quite thick and their imperfection values are generally small. Therefore, it is considered that data which belongs to $\Delta_o/t = 0.2$ is more representative of the behavior in this region.

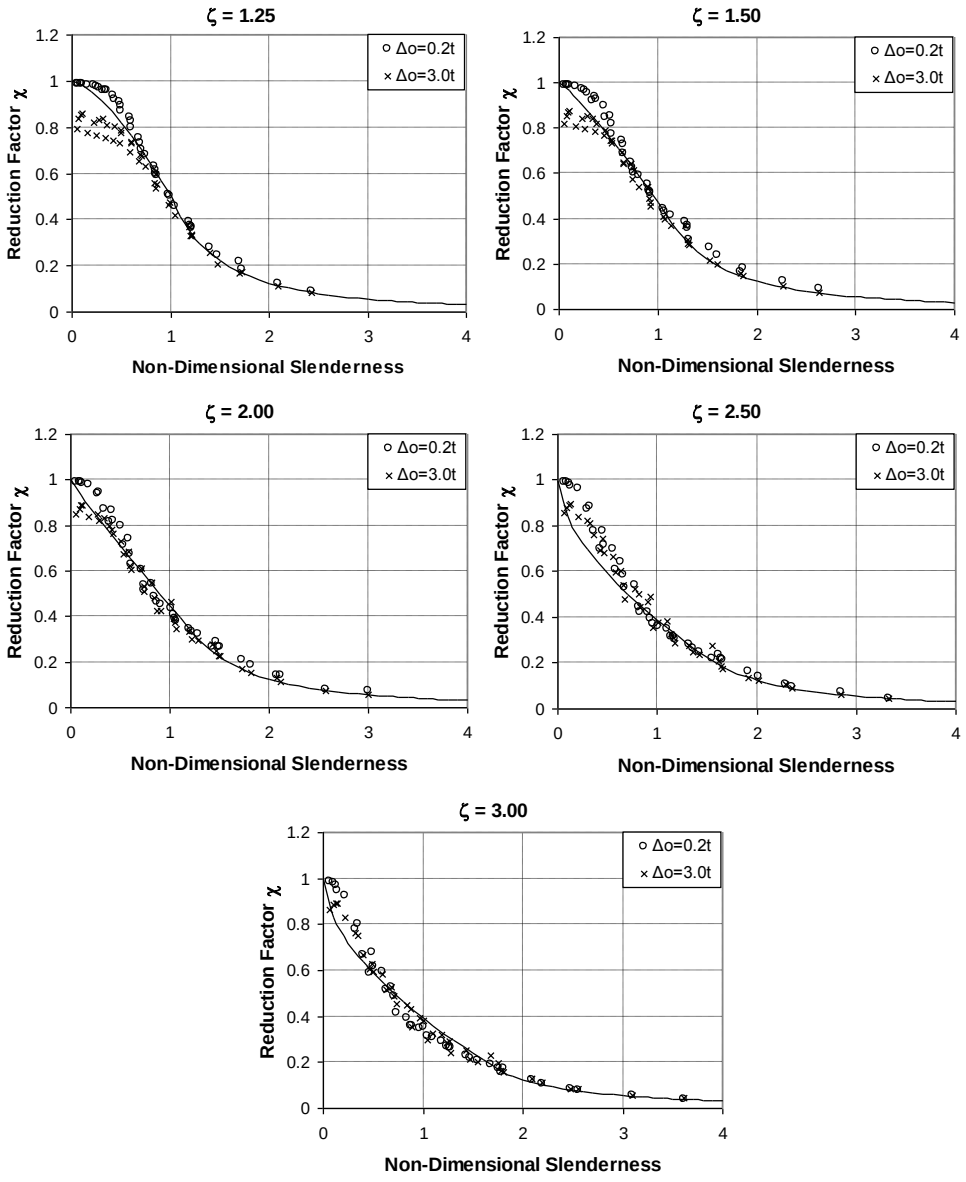

Figure 2.18: Proposed capacity curves and characteristic resistances based on GMNIA analyses

CHAPTER 3

CONCLUSIONS AND RECOMMENDATIONS

3.1 Conclusions and Recommendations for Future Research

A numerical study on buckling of cylindrical shells resting on discretely supported ring beams has been presented. Linear elastic analysis (LA), linear elastic bifurcation analysis (LBA), geometrically nonlinear elastic analysis (GNA), materially nonlinear analysis (MNA), geometrically and materially nonlinear analysis (GMNA), geometrically nonlinear elastic analysis with imperfections included (GNIA), and geometrically and materially nonlinear analysis with imperfections included (GMNIA) were conducted to systematically study the problem of interest. The following can be concluded based on the results of this numerical study:

- The linear elastic bifurcation analysis (LBA) results indicate that the LBA resistance can be estimated by dividing the classical elastic buckling stress for uniform compression by the stress ratio. More accurate estimates can be found using Equation 4.

- An elastic imperfection study which considered the eigenmode-affine imperfection pattern indicate that the buckling loads are relatively insensitive to amplitude of imperfection in the domain between $\Delta_o/t = 0.1$ and $\Delta_o/t = 3.0$. The imperfection sensitivity study revealed that direction of imperfections has influence on the results and both the inward and outward imperfections must be considered for an accurate assessment.

- The elastic imperfection and nonlinearity factor (α) was found to be equal to 0.5. Influences of geometrical effects and imperfections have a variable role on α, depending on r/t and stress ratio. In general, the geometrical effects are more pronounced as the r/t ratio decrease and stress ratio increases.

- The materially nonlinear analysis results indicate that the plastic collapse resistance reaches to the yield stress regardless of the stress ratio. Although cases with high stress ratios result in earlier yielding of the cylindrical shell, the resistances asymptotically reach to the yield stress.

- The results from geometrically and materially nonlinear analysis with imperfections, were used to generate resistance curves which depend on the MNA and LBA resistances. The parameters for the resistance curves were found to depend on the stress ratio and were found to be insensitive to r/t ratio. The proposed resistance curves can be used together with Equations 4 and 5 to determine the characteristic resistance. The developed procedure does not require GMNIA and only requires a linear finite element analysis to determine the stress ratio. The procedure offered by Topkaya and Rotter [19] can also be used to estimate the amount of stress ratio for a given shell and ring beam geometry.

Future research should consider parameters which were not investigated in this study. Other ring beam geometries and support widths require further consideration. More importantly are the shape and amplitude of imperfections. This study assumed an eigenmode-affine imperfection pattern according to the recommendations of EN 1993-1-6 [6]. Other imperfection patterns which may produce more deleterious effects should be explored.

REFERENCES

[1] Rotter, J.M. (2001) "Guide for the Economic Design of Circular Metal Silos", Spon, London.

[2] Wozniak, R.S. "Steel Tanks", Structural Engineering Handbook, 2nd edn, Section 23, Eds. E.H. and C.N. Gaylord, McGraw-Hill, New York, 1979.

[3] Trahair, N.S., Abel, A., Ansourian, P., Irvine, H.M. and Rotter, J.M. "Structural Design of Steel Bins for Bulk Solids", Australian Institute of Steel Construction, Sydney, 1983.

[4] Gaylord, E.H. and Gaylord, C.N. Design of Steel Bins for Storage of Bulk Solids, Prentice Hall, Englewood Cliffs, 1984.

[5] Safarian, S.S. and Harris, E.C. "Design and Construction of Silos and Bunkers", Van Nostrand Reinhold, New York, 1985.

[6] EN 1993-1-6 "Eurocode 3: Design of Steel Structures, Part-1-6: Strength and Stability of Shell Structures", European Committee for Standardization, Brussels, Belgium, 2007.

[7] Kildegaard, A. "Bending of a Cylindrical Shell subject to Axial Loading", 2nd Symp. Theory of Thin Shells, IUTAM, Springer, Berlin, 301-315, 1969

[8] Gould, P. L., Sen, S. K., Wang, R. S. C., Suryoutomo, H. and Lowrey, R. D. "Column Supported Cylindrical-Conical Tanks", J Struct. Div., ASCE, 102 (ST2), 429-447, 1976.

[9] Gould, P. L., Sen, S. K., Wang, R. S. C., Suryoutomo, H. and Lowrey, R. D. "Column Supported Cylindrical-Conical Tanks", J Struct. Div., ASCE, 102 (ST2), 429-447, 1976.

[10] Gould, P. L., Ravichandran, R.V. and Sridharan, S. "A local-global FE model for nonlinear analysis of column-supported shells of revolution", Thin-Walled Structures, 31, 25-37, 1998.

[11] Rotter, J.M. "Membrane Theory of Shells for Bins and Silos", Transactions of Mechanical Engineering, Institution of Engineers, Australia, Vol. ME12 No.3 September, pp 135-147, 1987.

[12] Rotter, J.M. "Structural Design of Light Gauge Silo Hoppers", Journal of Structural Engineering, ASCE, Vol. 116, No. 7, July 1990, pp 1907-1922, 1990.

[13] Teng, J.G., Rotter, J.M. "Linear bifurcation of perfect column-supported cylinders: Support modeling and boundary conditions." Thin-Walled Structures, 14(3) 241-263, 1992.

[14] Guggenberger, W., Greiner, R. and Rotter, J.M. "The Behaviour of Locally-Supported Cylindrical Shells: Unstiffened Shells", J. Constr. Steel Res., 56 (2) 175-197, 2000.

[15] Guggenberger, W. Greiner, R. and Rotter, J.M. "Cylindrical shells above local supports", in Buckling of Thin Metal Shells, eds J.G. Teng & J.M. Rotter, Spon, London, 88-128, 2004.

[16] Greiner, R. and Guggenberger, W. "Buckling Behaviour of Axially Loaded Steel Cylinders on Local Supports - with and without Internal Pressure", Thin Walled Structures, Vol. 31, pp 159-167, 1998.

[17] Rotter, J.M., Cai, M. and Holst, J.M.F.G. "Buckling of thin cylindrical shells under locally elevated axial compression stresses", Journal of Pressure Vessel Technology, Vol. 133, Issue 1, February, pp. 011204-1 to 11, 2011.

[18] Song, C.Y., Teng J.G. and Rotter J.M. "Imperfection sensitivity of thin elastic cylindrical shells subject to partial axial compression", International Journal of Solids and Structures, Vol. 41, pp 7155-7180, 2004.

[19] Topkaya, C., Rotter, J.M. "Ring beam stiffness criterion for column supported metal silos", ASCE Journal of Engineering Mechanics, 137(12) 846-853, 2011.

[20] ECCS "Stability of Steel Shells: European Design Recommendations: Fifth Edition 2008", Eds J.M. Rotter and H. Schmidt, Publication P125, European Convention for Constructional Steelwork, Brussels, 384 pp, 2008.

[21] Rotter, J.M. "Shell buckling and assessment and the LBA-MNA methodology" Stahlbau, Vol. 80, No. 11, pp. 791-803, 2011.

[22] Ansys 12.1 [Computer software], Canonsburg, PA, Ansys.

[23] Guggenberger, W. "Buckling of cylindrical shells under local axial loads" In Buckling of Shell Structures, on Land, in the Sea and in the Air, (ed. J.F. Jullien. International Colloquium, Villeurbanne, Lyon, France, 17-19 September, Elsevier Applied Science, pp. 323-333, 1991.

[24] Guggenberger, W. "Nonlinear buckling behavior of circular cylindrical shells under local axial loads" Doctoral Dissertation (in German), Institute for Steel, Timber and Shell Structures, Report No. 6, Technical University of Graz, Austria, 1992.

[25] She, K.M. and Rotter, J.M. "Nonlinear and stability behavior of discretely supported cylinders" Research Report 93-01, Department of Civil Engineering, University of Edinburgh, 1993.

[26] Lorenz, R. "Buckling of cylindrical shell under axial compression" Zeitschrift des Vereines Deutscher Ingenieure, 52, In German, 1908.

[27] Timoshenko, S.P. Einige Stabilitätsprobleme der Elasticitätsheorie. Zeitschrift für Mathematik und Physik 58, 378-385, 1910.

[28] Southwell, R.V. Philosophical Transactions of the Royal Society, 213, 187, 1914.

[29] Libai, A., Durban D. "Buckling of cylindrical shells subjected to non-uniform axial loads" Journal of Applied Mechanics, American Society of Mechanical Engineers, 44, 714-720, 1977.

[30] Rotter, J.M. "Buckling of Ground-Supported Cylindrical Steel Bins under Vertical Compressive Wall Loads", Proc., Metal Structures Conference, Institution of Engineers Australia, Melbourne, pp 112-127, 1985.

[31] Rotter, J.M. "A framework for exploiting different computational assessments in structural design" Proc. Sixth International Conference on Steel and Aluminum Structures, 6th ICSAS 07, Oxford, June 2007

APPENDIX A

ANALYSIS RESULTS

All produced data results are tabulated case by case; and they are available in the appendix below starting from the next page.

Explanations for the notations and abbreviations used in the tables:

Erb: Elastic Modulus of Ring Beam

Target ζ: Target Stress Ratio

Actual ζ: Actual Stress Ratio

El. Critic.: Elastic Critical Stress, calculated using Equation 1

worst: Result of the worst of the two analyses of inward and outward imperfection for that particular case.

Table A-1: Cases Considered in the Parametric Study, Elastic Critical Stress for Each Case and the Results of LBA and GNA for Each Case

Analysis Number	Case Number	Radius (r) mm	Thickness (t) mm	r/t	Erb GPa	Target ζ	Actual ζ	Yield Stress MPa	El. Critic. MPa	LBA MPa	GNA MPa
1	1	3000	3	1000	800	1.250	1.254	1	121.0	101.5	97.6
2	1	3000	3	1000	800	1.250	1.254	10	121.0	101.5	97.6
3	1	3000	3	1000	800	1.250	1.254	25	121.0	101.5	97.6
4	1	3000	3	1000	800	1.250	1.254	50	121.0	101.5	97.6
5	1	3000	3	1000	800	1.250	1.254	75	121.0	101.5	97.6
6	1	3000	3	1000	800	1.250	1.254	100	121.0	101.5	97.6
7	1	3000	3	1000	800	1.250	1.254	150	121.0	101.5	97.6
8	1	3000	3	1000	800	1.250	1.254	200	121.0	101.5	97.6
9	1	3000	3	1000	800	1.250	1.254	300	121.0	101.5	97.6
10	1	3000	3	1000	800	1.250	1.254	600	121.0	101.5	97.6
11	2	3000	3	1000	360	1.500	1.499	1	121.0	86.7	83.6
12	2	3000	3	1000	360	1.500	1.499	10	121.0	86.7	83.6
13	2	3000	3	1000	360	1.500	1.499	25	121.0	86.7	83.6
14	2	3000	3	1000	360	1.500	1.499	50	121.0	86.7	83.6
15	2	3000	3	1000	360	1.500	1.499	75	121.0	86.7	83.6
16	2	3000	3	1000	360	1.500	1.499	100	121.0	86.7	83.6
17	2	3000	3	1000	360	1.500	1.499	150	121.0	86.7	83.6
18	2	3000	3	1000	360	1.500	1.499	200	121.0	86.7	83.6
19	2	3000	3	1000	360	1.500	1.499	300	121.0	86.7	83.6
20	2	3000	3	1000	360	1.500	1.499	600	121.0	86.7	83.6
21	3	3000	3	1000	134	2.000	2.007	1	121.0	66.6	63.1
22	3	3000	3	1000	134	2.000	2.007	10	121.0	66.6	63.1

Table A-1 cont'd

Analysis Number	Case Number	Radius (r) mm	Thickness (t) mm	r/t	Erb GPa	Target ζ	Actual ζ	Yield Stress MPa	El. Critic. MPa	LBA MPa	GNA MPa
23	3	3000	3	1000	134	2.000	2.007	25	121.0	66.6	63.1
24	3	3000	3	1000	134	2.000	2.007	50	121.0	66.6	63.1
25	3	3000	3	1000	134	2.000	2.007	75	121.0	66.6	63.1
26	3	3000	3	1000	134	2.000	2.007	100	121.0	66.6	63.1
27	3	3000	3	1000	134	2.000	2.007	150	121.0	66.6	63.1
28	3	3000	3	1000	134	2.000	2.007	200	121.0	66.6	63.1
29	3	3000	3	1000	134	2.000	2.007	300	121.0	66.6	63.1
30	3	3000	3	1000	134	2.000	2.007	600	121.0	66.6	63.1
31	4	3000	3	1000	64	2.500	2.506	1	121.0	54.3	49.0
32	4	3000	3	1000	64	2.500	2.506	10	121.0	54.3	49.0
33	4	3000	3	1000	64	2.500	2.506	25	121.0	54.3	49.0
34	4	3000	3	1000	64	2.500	2.506	50	121.0	54.3	49.0
35	4	3000	3	1000	64	2.500	2.506	75	121.0	54.3	49.0
36	4	3000	3	1000	64	2.500	2.506	100	121.0	54.3	49.0
37	4	3000	3	1000	64	2.500	2.506	150	121.0	54.3	49.0
38	4	3000	3	1000	64	2.500	2.506	200	121.0	54.3	49.0
39	4	3000	3	1000	64	2.500	2.506	300	121.0	54.3	49.0
40	4	3000	3	1000	64	2.500	2.506	600	121.0	54.3	49.0
41	5	3000	3	1000	32	3.000	3.008	1	121.0	46.0	39.9
42	5	3000	3	1000	32	3.000	3.008	10	121.0	46.0	39.9
43	5	3000	3	1000	32	3.000	3.008	25	121.0	46.0	39.9
44	5	3000	3	1000	32	3.000	3.008	50	121.0	46.0	39.9
45	5	3000	3	1000	32	3.000	3.008	75	121.0	46.0	39.9

Table A-1 cont'd

Analysis Number	Case Number	Radius (r) mm	Thickness (t) mm	r/t	Erb GPa	Target ζ	Actual ζ	Yield Stress MPa	El. Critic. MPa	LBA MPa	GNA MPa
46	5	3000	3	1000	32	3.000	3.008	100	121.0	46.0	39.9
47	5	3000	3	1000	32	3.000	3.008	150	121.0	46.0	39.9
48	5	3000	3	1000	32	3.000	3.008	200	121.0	46.0	39.9
49	5	3000	3	1000	32	3.000	3.008	300	121.0	46.0	39.9
50	5	3000	4	750	32	3.000	3.008	600	161.3	46.0	39.9
51	6	3000	4	750	1100	1.250	1.250	1	161.3	136.5	131.1
52	6	3000	4	750	1100	1.250	1.250	10	161.3	136.5	131.1
53	6	3000	4	750	1100	1.250	1.250	25	161.3	136.5	131.1
54	6	3000	4	750	1100	1.250	1.250	50	161.3	136.5	131.1
55	6	3000	4	750	1100	1.250	1.250	75	161.3	136.5	131.1
56	6	3000	4	750	1100	1.250	1.250	100	161.3	136.5	131.1
57	6	3000	4	750	1100	1.250	1.250	150	161.3	136.5	131.1
58	6	3000	4	750	1100	1.250	1.250	200	161.3	136.5	131.1
59	6	3000	4	750	1100	1.250	1.250	300	161.3	136.5	131.1
60	6	3000	4	750	1100	1.250	1.250	600	161.3	136.5	131.1
61	7	3000	4	750	488	1.500	1.500	1	161.3	116.7	112.9
62	7	3000	4	750	488	1.500	1.500	10	161.3	116.7	112.9
63	7	3000	4	750	488	1.500	1.500	25	161.3	116.7	112.9
64	7	3000	4	750	488	1.500	1.500	50	161.3	116.7	112.9
65	7	3000	4	750	488	1.500	1.500	75	161.3	116.7	112.9
66	7	3000	4	750	488	1.500	1.500	100	161.3	116.7	112.9
67	7	3000	4	750	488	1.500	1.500	150	161.3	116.7	112.9
68	7	3000	4	750	488	1.500	1.500	200	161.3	116.7	112.9

Table A-1 cont'd

Analysis Number	Case Number	Radius (r) mm	Thickness (t) mm	r/t	Erb GPa	Target ζ	Actual ζ	Yield Stress MPa	El. Critic. MPa	LBA MPa	GNA MPa
69	7	3000	4	750	488	1.500	1.500	300	161.3	116.7	112.9
70	7	3000	4	750	488	1.500	1.500	600	161.3	116.7	112.9
71	8	3000	4	750	184	2.000	1.998	1	161.3	90.3	82.7
72	8	3000	4	750	184	2.000	1.998	10	161.3	90.3	82.7
73	8	3000	4	750	184	2.000	1.998	25	161.3	90.3	82.7
74	8	3000	4	750	184	2.000	1.998	50	161.3	90.3	82.7
75	8	3000	4	750	184	2.000	1.998	75	161.3	90.3	82.7
76	8	3000	4	750	184	2.000	1.998	100	161.3	90.3	82.7
77	8	3000	4	750	184	2.000	1.998	150	161.3	90.3	82.7
78	8	3000	4	750	184	2.000	1.998	200	161.3	90.3	82.7
79	8	3000	4	750	184	2.000	1.998	300	161.3	90.3	82.7
80	8	3000	4	750	184	2.000	1.998	600	161.3	90.3	82.7
81	9	3000	4	750	89	2.500	2.502	1	161.3	73.8	64.2
82	9	3000	4	750	89	2.500	2.502	10	161.3	73.8	64.2
83	9	3000	4	750	89	2.500	2.502	25	161.3	73.8	64.2
84	9	3000	4	750	89	2.500	2.502	50	161.3	73.8	64.2
85	9	3000	4	750	89	2.500	2.502	75	161.3	73.8	64.2
86	9	3000	4	750	89	2.500	2.502	100	161.3	73.8	64.2
87	9	3000	4	750	89	2.500	2.502	150	161.3	73.8	64.2
88	9	3000	4	750	89	2.500	2.502	200	161.3	73.8	64.2
89	9	3000	4	750	89	2.500	2.502	300	161.3	73.8	64.2
90	9	3000	4	750	89	2.500	2.502	600	161.3	73.8	64.2
91	10	3000	4	750	45	3.000	3.004	1	161.3	62.6	51.6

Table A-1 cont'd

Analysis Number	Case Number	Radius (r) mm	Thickness (t) mm	r/t	Erb GPa	Target ζ	Actual ζ	Yield Stress MPa	El. Critic. MPa	LBA MPa	GNA MPa
92	10	3000	4	750	45	3.000	3.004	10	161.3	62.6	51.6
93	10	3000	4	750	45	3.000	3.004	25	161.3	62.6	51.6
94	10	3000	4	750	45	3.000	3.004	50	161.3	62.6	51.6
95	10	3000	4	750	45	3.000	3.004	75	161.3	62.6	51.6
96	10	3000	4	750	45	3.000	3.004	100	161.3	62.6	51.6
97	10	3000	4	750	45	3.000	3.004	150	161.3	62.6	51.6
98	10	3000	4	750	45	3.000	3.004	200	161.3	62.6	51.6
99	10	3000	4	750	45	3.000	3.004	300	161.3	62.6	51.6
100	10	3000	4	750	45	3.000	3.004	600	161.3	62.6	51.6
101	11	3000	6	500	1700	1.250	1.249	1	242.0	207.3	195.9
102	11	3000	6	500	1700	1.250	1.249	10	242.0	207.3	195.9
103	11	3000	6	500	1700	1.250	1.249	25	242.0	207.3	195.9
104	11	3000	6	500	1700	1.250	1.249	50	242.0	207.3	195.9
105	11	3000	6	500	1700	1.250	1.249	75	242.0	207.3	195.9
106	11	3000	6	500	1700	1.250	1.249	100	242.0	207.3	195.9
107	11	3000	6	500	1700	1.250	1.249	150	242.0	207.3	195.9
108	11	3000	6	500	1700	1.250	1.249	200	242.0	207.3	195.9
109	11	3000	6	500	1700	1.250	1.249	300	242.0	207.3	195.9
110	11	3000	6	500	1700	1.250	1.249	600	242.0	207.3	195.9
111	12	3000	6	500	760	1.500	1.497	1	242.0	178.5	164.2
112	12	3000	6	500	760	1.500	1.497	10	242.0	178.5	164.2
113	12	3000	6	500	760	1.500	1.497	25	242.0	178.5	164.2
114	12	3000	6	500	760	1.500	1.497	50	242.0	178.5	164.2

Table A-1 cont'd

Analysis Number	Case Number	Radius (r) mm	Thickness (t) mm	r/t	Erb GPa	Target ζ	Actual ζ	Yield Stress MPa	El. Critic. MPa	LBA MPa	GNA MPa
115	12	3000	6	500	760	1.500	1.497	75	242.0	178.5	164.2
116	12	3000	6	500	760	1.500	1.497	100	242.0	178.5	164.2
117	12	3000	6	500	760	1.500	1.497	150	242.0	178.5	164.2
118	12	3000	6	500	760	1.500	1.497	200	242.0	178.5	164.2
119	12	3000	6	500	760	1.500	1.497	300	242.0	178.5	164.2
120	12	3000	6	500	760	1.500	1.497	600	242.0	178.5	164.2
121	13	3000	6	500	290	2.000	2.002	1	242.0	138.9	122.8
122	13	3000	6	500	290	2.000	2.002	10	242.0	138.9	122.8
123	13	3000	6	500	290	2.000	2.002	25	242.0	138.9	122.8
124	13	3000	6	500	290	2.000	2.002	50	242.0	138.9	122.8
125	13	3000	6	500	290	2.000	2.002	75	242.0	138.9	122.8
126	13	3000	6	500	290	2.000	2.002	100	242.0	138.9	122.8
127	13	3000	6	500	290	2.000	2.002	150	242.0	138.9	122.8
128	13	3000	6	500	290	2.000	2.002	200	242.0	138.9	122.8
129	13	3000	6	500	290	2.000	2.002	300	242.0	138.9	122.8
130	13	3000	6	500	290	2.000	2.002	600	242.0	138.9	122.8
131	14	3000	6	500	142	2.500	2.502	1	242.0	114.4	95.4
132	14	3000	6	500	142	2.500	2.502	10	242.0	114.4	95.4
133	14	3000	6	500	142	2.500	2.502	25	242.0	114.4	95.4
134	14	3000	6	500	142	2.500	2.502	50	242.0	114.4	95.4
135	14	3000	6	500	142	2.500	2.502	75	242.0	114.4	95.4
136	14	3000	6	500	142	2.500	2.502	100	242.0	114.4	95.4
137	14	3000	6	500	142	2.500	2.502	150	242.0	114.4	95.4

Table A-1 cont'd

Analysis Number	Case Number	Radius (r) mm	Thickness (t) mm	r/t	Erb GPa	Target ζ	Actual ζ	Yield Stress MPa	El. Critic. MPa	LBA MPa	GNA MPa
138	14	3000	6	500	142	2.500	2.502	200	242.0	114.4	95.4
139	14	3000	6	500	142	2.500	2.502	300	242.0	114.4	95.4
140	14	3000	6	500	142	2.500	2.502	600	242.0	114.4	95.4
141	15	3000	6	500	74	3.000	2.994	1	242.0	97.8	76.3
142	15	3000	6	500	74	3.000	2.994	10	242.0	97.8	76.3
143	15	3000	6	500	74	3.000	2.994	25	242.0	97.8	76.3
144	15	3000	6	500	74	3.000	2.994	50	242.0	97.8	76.3
145	15	3000	6	500	74	3.000	2.994	75	242.0	97.8	76.3
146	15	3000	6	500	74	3.000	2.994	100	242.0	97.8	76.3
147	15	3000	6	500	74	3.000	2.994	150	242.0	97.8	76.3
148	15	3000	6	500	74	3.000	2.994	200	242.0	97.8	76.3
149	15	3000	6	500	74	3.000	2.994	300	242.0	97.8	76.3
150	15	3000	6	500	74	3.000	2.994	600	242.0	97.8	76.3
151	16	3000	12	250	3600	1.250	1.250	1	484.0	425.7	387.2
152	16	3000	12	250	3600	1.250	1.250	10	484.0	425.7	387.2
153	16	3000	12	250	3600	1.250	1.250	25	484.0	425.7	387.2
154	16	3000	12	250	3600	1.250	1.250	50	484.0	425.7	387.2
155	16	3000	12	250	3600	1.250	1.250	75	484.0	425.7	387.2
156	16	3000	12	250	3600	1.250	1.250	100	484.0	425.7	387.2
157	16	3000	12	250	3600	1.250	1.250	150	484.0	425.7	387.2
158	16	3000	12	250	3600	1.250	1.250	200	484.0	425.7	387.2
159	16	3000	12	250	3600	1.250	1.250	300	484.0	425.7	387.2
160	16	3000	12	250	3600	1.250	1.250	600	484.0	425.7	387.2

Table A-1 cont'd

Analysis Number	Case Number	Radius (r) mm	Thickness (t) mm	r/t	Erb GPa	Target ζ	Actual ζ	Yield Stress MPa	El. Critic. MPa	LBA MPa	GNA MPa
161	17	3000	12	250	1600	1.500	1.504	1	484.0	371.1	317.6
162	17	3000	12	250	1600	1.500	1.504	10	484.0	371.1	317.6
163	17	3000	12	250	1600	1.500	1.504	25	484.0	371.1	317.6
164	17	3000	12	250	1600	1.500	1.504	50	484.0	371.1	317.6
165	17	3000	12	250	1600	1.500	1.504	75	484.0	371.1	317.6
166	17	3000	12	250	1600	1.500	1.504	100	484.0	371.1	317.6
167	17	3000	12	250	1600	1.500	1.504	150	484.0	371.1	317.6
168	17	3000	12	250	1600	1.500	1.504	200	484.0	371.1	317.6
169	17	3000	12	250	1600	1.500	1.504	300	484.0	371.1	317.6
170	17	3000	12	250	1600	1.500	1.504	600	484.0	371.1	317.6
171	18	3000	12	250	630	2.000	2.006	1	484.0	295.3	232.2
172	18	3000	12	250	630	2.000	2.006	10	484.0	295.3	232.2
173	18	3000	12	250	630	2.000	2.006	25	484.0	295.3	232.2
174	18	3000	12	250	630	2.000	2.006	50	484.0	295.3	232.2
175	18	3000	12	250	630	2.000	2.006	75	484.0	295.3	232.2
176	18	3000	12	250	630	2.000	2.006	100	484.0	295.3	232.2
177	18	3000	12	250	630	2.000	2.006	150	484.0	295.3	232.2
178	18	3000	12	250	630	2.000	2.006	200	484.0	295.3	232.2
179	18	3000	12	250	630	2.000	2.006	300	484.0	295.3	232.2
180	18	3000	12	250	630	2.000	2.006	600	484.0	295.3	232.2
181	19	3000	12	250	318	2.500	2.501	1	484.0	246.7	181.8
182	19	3000	12	250	318	2.500	2.501	10	484.0	246.7	181.8
183	19	3000	12	250	318	2.500	2.501	25	484.0	246.7	181.8

Table A-1 cont'd

Analysis Number	Case Number	Radius (r) mm	Thickness (t) mm	r/t	Erb GPa	Target ζ	Actual ζ	Yield Stress MPa	El. Critic. MPa	LBA MPa	GNA MPa
184	19	3000	12	250	318	2.500	2.501	50	484.0	246.7	181.8
185	19	3000	12	250	318	2.500	2.501	75	484.0	246.7	181.8
186	19	3000	12	250	318	2.500	2.501	100	484.0	246.7	181.8
187	19	3000	12	250	318	2.500	2.501	150	484.0	246.7	181.8
188	19	3000	12	250	318	2.500	2.501	200	484.0	246.7	181.8
189	19	3000	12	250	318	2.500	2.501	300	484.0	246.7	181.8
190	19	3000	12	250	318	2.500	2.501	600	484.0	246.7	181.8
191	20	3000	12	250	168	3.000	3.001	1	484.0	212.2	142.5
192	20	3000	12	250	168	3.000	3.001	10	484.0	212.2	142.5
193	20	3000	12	250	168	3.000	3.001	25	484.0	212.2	142.5
194	20	3000	12	250	168	3.000	3.001	50	484.0	212.2	142.5
195	20	3000	12	250	168	3.000	3.001	75	484.0	212.2	142.5
196	20	3000	12	250	168	3.000	3.001	100	484.0	212.2	142.5
197	20	3000	12	250	168	3.000	3.001	150	484.0	212.2	142.5
198	20	3000	12	250	168	3.000	3.001	200	484.0	212.2	142.5
199	20	3000	12	250	168	3.000	3.001	300	484.0	212.2	142.5
200	20	3000	12	250	168	3.000	3.001	600	484.0	212.2	142.5

Table A-2: GNIA Results for 0.1t, 0.2t, 0.5t and 1t Imperfection Cases

	GNIA 0.1t	GNIA 0.1t	GNIA 0.1t	GNIA 0.2t	GNIA 0.2t	GNIA 0.2t	GNIA 0.5t	GNIA 0.5t	GNIA 0.5t	GNIA 1t	GNIA 1t	GNIA 1t
Analysis	**inward**	**outward**	**worst**	**inward**	**outward**	**worst**	**inward**	**outward**	**worst**	**inward**	**outward**	**worst**
Number	**MPa**	**MPa**	**MPa**	**MPa**	**MPa**	**MPa**	**MPa**	**MPa**	**MPa**	**MPa**	**MPa**	**MPa**
1	65.1	65.7	65.1	54.8	55.6	54.8	61.4	68.0	61.4	57.7	59.0	57.7
2	65.1	65.7	65.1	54.8	55.6	54.8	61.4	68.0	61.4	57.7	59.0	57.7
3	65.1	65.7	65.1	54.8	55.6	54.8	61.4	68.0	61.4	57.7	59.0	57.7
4	65.1	65.7	65.1	54.8	55.6	54.8	61.4	68.0	61.4	57.7	59.0	57.7
5	65.1	65.7	65.1	54.8	55.6	54.8	61.4	68.0	61.4	57.7	59.0	57.7
6	65.1	65.7	65.1	54.8	55.6	54.8	61.4	68.0	61.4	57.7	59.0	57.7
7	65.1	65.7	65.1	54.8	55.6	54.8	61.4	68.0	61.4	57.7	59.0	57.7
8	65.1	65.7	65.1	54.8	55.6	54.8	61.4	68.0	61.4	57.7	59.0	57.7
9	65.1	65.7	65.1	54.8	55.6	54.8	61.4	68.0	61.4	57.7	59.0	57.7
10	65.1	65.7	65.1	54.8	55.6	54.8	61.4	68.0	61.4	57.7	59.0	57.7
11	55.9	55.9	55.9	58.1	55.3	55.3	55.3	59.9	55.3	50.2	50.8	50.2
12	55.9	55.9	55.9	58.1	55.3	55.3	55.3	59.9	55.3	50.2	50.8	50.2
13	55.9	55.9	55.9	58.1	55.3	55.3	55.3	59.9	55.3	50.2	50.8	50.2
14	55.9	55.9	55.9	58.1	55.3	55.3	55.3	59.9	55.3	50.2	50.8	50.2
15	55.9	55.9	55.9	58.1	55.3	55.3	55.3	59.9	55.3	50.2	50.8	50.2
16	55.9	55.9	55.9	58.1	55.3	55.3	55.3	59.9	55.3	50.2	50.8	50.2
17	55.9	55.9	55.9	58.1	55.3	55.3	55.3	59.9	55.3	50.2	50.8	50.2
18	55.9	55.9	55.9	58.1	55.3	55.3	55.3	59.9	55.3	50.2	50.8	50.2
19	55.9	55.9	55.9	58.1	55.3	55.3	55.3	59.9	55.3	50.2	50.8	50.2
20	55.9	55.9	55.9	58.1	55.3	55.3	55.3	59.9	55.3	50.2	50.8	50.2
21	50.9	38.6	38.6	47.7	43.2	43.2	45.5	46.8	45.5	35.4	42.8	35.4

Table A-2 cont'd

	GNIA 0.1t	GNIA 0.1t	GNIA 0.1t	GNIA 0.2t	GNIA 0.2t	GNIA 0.2t	GNIA 0.5t	GNIA 0.5t	GNIA 0.5t	GNIA 1t	GNIA 1t	GNIA 1t
Analysis	**inward**	**outward**	**worst**	**inward**	**outward**	**worst**	**inward**	**outward**	**worst**	**inward**	**outward**	**worst**
Number	**MPa**	**MPa**	**MPa**	**MPa**	**MPa**	**MPa**	**MPa**	**MPa**	**MPa**	**MPa**	**MPa**	**MPa**
22	50.9	38.6	38.6	47.7	43.2	43.2	45.5	46.8	45.5	35.4	42.8	35.4
23	50.9	38.6	38.6	47.7	43.2	43.2	45.5	46.8	45.5	35.4	42.8	35.4
24	50.9	38.6	38.6	47.7	43.2	43.2	45.5	46.8	45.5	35.4	42.8	35.4
25	50.9	38.6	38.6	47.7	43.2	43.2	45.5	46.8	45.5	35.4	42.8	35.4
26	50.9	38.6	38.6	47.7	43.2	43.2	45.5	46.8	45.5	35.4	42.8	35.4
27	50.9	38.6	38.6	47.7	43.2	43.2	45.5	46.8	45.5	35.4	42.8	35.4
28	50.9	38.6	38.6	47.7	43.2	43.2	45.5	46.8	45.5	35.4	42.8	35.4
29	50.9	38.6	38.6	47.7	43.2	43.2	45.5	46.8	45.5	35.4	42.8	35.4
30	50.9	38.6	38.6	47.7	43.2	43.2	45.5	46.8	45.5	35.4	42.8	35.4
31	33.0	31.2	31.2	28.7	32.2	28.7	39.6	37.2	37.2	38.7	34.3	34.3
32	33.0	31.2	31.2	28.7	32.2	28.7	39.6	37.2	37.2	38.7	34.3	34.3
33	33.0	31.2	31.2	28.7	32.2	28.7	39.6	37.2	37.2	38.7	34.3	34.3
34	33.0	31.2	31.2	28.7	32.2	28.7	39.6	37.2	37.2	38.7	34.3	34.3
35	33.0	31.2	31.2	28.7	32.2	28.7	39.6	37.2	37.2	38.7	34.3	34.3
36	33.0	31.2	31.2	28.7	32.2	28.7	39.6	37.2	37.2	38.7	34.3	34.3
37	33.0	31.2	31.2	28.7	32.2	28.7	39.6	37.2	37.2	38.7	34.3	34.3
38	33.0	31.2	31.2	28.7	32.2	28.7	39.6	37.2	37.2	38.7	34.3	34.3
39	33.0	31.2	31.2	28.7	32.2	28.7	39.6	37.2	37.2	38.7	34.3	34.3
40	33.0	31.2	31.2	28.7	32.2	28.7	39.6	37.2	37.2	38.7	34.3	34.3
41	28.3	28.3	28.3	27.4	24.2	24.2	31.1	27.8	27.8	28.2	34.0	28.2
42	28.3	28.3	28.3	27.4	24.2	24.2	31.1	27.8	27.8	28.2	34.0	28.2

Table A-2 cont'd

	GNIA 0.1t	GNIA 0.1t	GNIA 0.1t	GNIA 0.2t	GNIA 0.2t	GNIA 0.2t	GNIA 0.5t	GNIA 0.5t	GNIA 0.5t	GNIA 1t	GNIA 1t	GNIA 1t
Analysis	**inward**	**outward**	**worst**	**inward**	**outward**	**worst**	**inward**	**outward**	**worst**	**inward**	**outward**	**worst**
Number	**MPa**	**MPa**	**MPa**	**MPa**	**MPa**	**MPa**	**MPa**	**MPa**	**MPa**	**MPa**	**MPa**	**MPa**
43	28.3	28.3	28.3	27.4	24.2	24.2	31.1	27.8	27.8	28.2	34.0	28.2
44	28.3	28.3	28.3	27.4	24.2	24.2	31.1	27.8	27.8	28.2	34.0	28.2
45	28.3	28.3	28.3	27.4	24.2	24.2	31.1	27.8	27.8	28.2	34.0	28.2
46	28.3	28.3	28.3	27.4	24.2	24.2	31.1	27.8	27.8	28.2	34.0	28.2
47	28.3	28.3	28.3	27.4	24.2	24.2	31.1	27.8	27.8	28.2	34.0	28.2
48	28.3	28.3	28.3	27.4	24.2	24.2	31.1	27.8	27.8	28.2	34.0	28.2
49	28.3	28.3	28.3	27.4	24.2	24.2	31.1	27.8	27.8	28.2	34.0	28.2
50	28.3	28.3	28.3	27.4	24.2	24.2	31.1	27.8	27.8	28.2	34.0	28.2
51	89.7	87.3	87.3	74.2	87.5	74.2	89.5	87.5	87.5	78.9	77.1	77.1
52	89.7	87.3	87.3	74.2	87.5	74.2	89.5	87.5	87.5	78.9	77.1	77.1
53	89.7	87.3	87.3	74.2	87.5	74.2	89.5	87.5	87.5	78.9	77.1	77.1
54	89.7	87.3	87.3	74.2	87.5	74.2	89.5	87.5	87.5	78.9	77.1	77.1
55	89.7	87.3	87.3	74.2	87.5	74.2	89.5	87.5	87.5	78.9	77.1	77.1
56	89.7	87.3	87.3	74.2	87.5	74.2	89.5	87.5	87.5	78.9	77.1	77.1
57	89.7	87.3	87.3	74.2	87.5	74.2	89.5	87.5	87.5	78.9	77.1	77.1
58	89.7	87.3	87.3	74.2	87.5	74.2	89.5	87.5	87.5	78.9	77.1	77.1
59	89.7	87.3	87.3	74.2	87.5	74.2	89.5	87.5	87.5	78.9	77.1	77.1
60	89.7	87.3	87.3	74.2	87.5	74.2	89.5	87.5	87.5	78.9	77.1	77.1
61	74.3	79.0	74.3	79.1	74.0	74.0	82.2	81.2	81.2	71.6	67.1	67.1
62	74.3	79.0	74.3	79.1	74.0	74.0	82.2	81.2	81.2	71.6	67.1	67.1
63	74.3	79.0	74.3	79.1	74.0	74.0	82.2	81.2	81.2	71.6	67.1	67.1

Table A-2 cont'd

	GNIA 0.1t	GNIA 0.1t	GNIA 0.1t	GNIA 0.2t	GNIA 0.2t	GNIA 0.2t	GNIA 0.5t	GNIA 0.5t	GNIA 0.5t	GNIA 1t	GNIA 1t	GNIA 1t
Analysis	**inward**	**outward**	**worst**	**inward**	**outward**	**worst**	**inward**	**outward**	**worst**	**inward**	**outward**	**worst**
Number	**MPa**	**MPa**	**MPa**	**MPa**	**MPa**	**MPa**	**MPa**	**MPa**	**MPa**	**MPa**	**MPa**	**MPa**
64	74.3	79.0	74.3	79.1	74.0	74.0	82.2	81.2	81.2	71.6	67.1	67.1
65	74.3	79.0	74.3	79.1	74.0	74.0	82.2	81.2	81.2	71.6	67.1	67.1
66	74.3	79.0	74.3	79.1	74.0	74.0	82.2	81.2	81.2	71.6	67.1	67.1
67	74.3	79.0	74.3	79.1	74.0	74.0	82.2	81.2	81.2	71.6	67.1	67.1
68	74.3	79.0	74.3	79.1	74.0	74.0	82.2	81.2	81.2	71.6	67.1	67.1
69	74.3	79.0	74.3	79.1	74.0	74.0	82.2	81.2	81.2	71.6	67.1	67.1
70	74.3	79.0	74.3	79.1	74.0	74.0	82.2	81.2	81.2	71.6	67.1	67.1
71	56.0	51.5	51.5	48.5	57.2	48.5	59.4	64.4	59.4	68.0	54.3	54.3
72	56.0	51.5	51.5	48.5	57.2	48.5	59.4	64.4	59.4	68.0	54.3	54.3
73	56.0	51.5	51.5	48.5	57.2	48.5	59.4	64.4	59.4	68.0	54.3	54.3
74	56.0	51.5	51.5	48.5	57.2	48.5	59.4	64.4	59.4	68.0	54.3	54.3
75	56.0	51.5	51.5	48.5	57.2	48.5	59.4	64.4	59.4	68.0	54.3	54.3
76	56.0	51.5	51.5	48.5	57.2	48.5	59.4	64.4	59.4	68.0	54.3	54.3
77	56.0	51.5	51.5	48.5	57.2	48.5	59.4	64.4	59.4	68.0	54.3	54.3
78	56.0	51.5	51.5	48.5	57.2	48.5	59.4	64.4	59.4	68.0	54.3	54.3
79	56.0	51.5	51.5	48.5	57.2	48.5	59.4	64.4	59.4	68.0	54.3	54.3
80	56.0	51.5	51.5	48.5	57.2	48.5	59.4	64.4	59.4	68.0	54.3	54.3
81	44.0	47.1	44.0	48.2	42.7	42.7	54.8	49.6	49.6	50.7	45.5	45.5
82	44.0	47.1	44.0	48.2	42.7	42.7	54.8	49.6	49.6	50.7	45.5	45.5
83	44.0	47.1	44.0	48.2	42.7	42.7	54.8	49.6	49.6	50.7	45.5	45.5
84	44.0	47.1	44.0	48.2	42.7	42.7	54.8	49.6	49.6	50.7	45.5	45.5

Table A-2 cont'd

	GNIA 0.1t	GNIA 0.1t	GNIA 0.1t	GNIA 0.2t	GNIA 0.2t	GNIA 0.2t	GNIA 0.5t	GNIA 0.5t	GNIA 0.5t	GNIA 1t	GNIA 1t	GNIA 1t
Analysis	**inward**	**outward**	**worst**	**inward**	**outward**	**worst**	**inward**	**outward**	**worst**	**inward**	**outward**	**worst**
Number	**MPa**	**MPa**	**MPa**	**MPa**	**MPa**	**MPa**	**MPa**	**MPa**	**MPa**	**MPa**	**MPa**	**MPa**
85	44.0	47.1	44.0	48.2	42.7	42.7	54.8	49.6	49.6	50.7	45.5	45.5
86	44.0	47.1	44.0	48.2	42.7	42.7	54.8	49.6	49.6	50.7	45.5	45.5
87	44.0	47.1	44.0	48.2	42.7	42.7	54.8	49.6	49.6	50.7	45.5	45.5
88	44.0	47.1	44.0	48.2	42.7	42.7	54.8	49.6	49.6	50.7	45.5	45.5
89	44.0	47.1	44.0	48.2	42.7	42.7	54.8	49.6	49.6	50.7	45.5	45.5
90	44.0	47.1	44.0	48.2	42.7	42.7	54.8	49.6	49.6	50.7	45.5	45.5
91	34.8	38.2	34.8	36.3	32.6	32.6	41.4	37.1	37.1	46.7	42.8	42.8
92	34.8	38.2	34.8	36.3	32.6	32.6	41.4	37.1	37.1	46.7	42.8	42.8
93	34.8	38.2	34.8	36.3	32.6	32.6	41.4	37.1	37.1	46.7	42.8	42.8
94	34.8	38.2	34.8	36.3	32.6	32.6	41.4	37.1	37.1	46.7	42.8	42.8
95	34.8	38.2	34.8	36.3	32.6	32.6	41.4	37.1	37.1	46.7	42.8	42.8
96	34.8	38.2	34.8	36.3	32.6	32.6	41.4	37.1	37.1	46.7	42.8	42.8
97	34.8	38.2	34.8	36.3	32.6	32.6	41.4	37.1	37.1	46.7	42.8	42.8
98	34.8	38.2	34.8	36.3	32.6	32.6	41.4	37.1	37.1	46.7	42.8	42.8
99	34.8	38.2	34.8	36.3	32.6	32.6	41.4	37.1	37.1	46.7	42.8	42.8
100	34.8	38.2	34.8	36.3	32.6	32.6	41.4	37.1	37.1	46.7	42.8	42.8
101	131.0	131.1	131.0	138.7	130.1	130.1	136.4	134.6	134.6	116.7	120.2	116.7
102	131.0	131.1	131.0	138.7	130.1	130.1	136.4	134.6	134.6	116.7	120.2	116.7
103	131.0	131.1	131.0	138.7	130.1	130.1	136.4	134.6	134.6	116.7	120.2	116.7
104	131.0	131.1	131.0	138.7	130.1	130.1	136.4	134.6	134.6	116.7	120.2	116.7
105	131.0	131.1	131.0	138.7	130.1	130.1	136.4	134.6	134.6	116.7	120.2	116.7

Table A-2 cont'd

	GNIA 0.1t	GNIA 0.1t	GNIA 0.1t	GNIA 0.2t	GNIA 0.2t	GNIA 0.2t	GNIA 0.5t	GNIA 0.5t	GNIA 0.5t	GNIA 1t	GNIA 1t	GNIA 1t
Analysis	**inward**	**outward**	**worst**	**inward**	**outward**	**worst**	**inward**	**outward**	**worst**	**inward**	**outward**	**worst**
Number	**MPa**	**MPa**	**MPa**	**MPa**	**MPa**	**MPa**	**MPa**	**MPa**	**MPa**	**MPa**	**MPa**	**MPa**
106	131.0	131.1	131.0	138.7	130.1	130.1	136.4	134.6	134.6	116.7	120.2	116.7
107	131.0	131.1	131.0	138.7	130.1	130.1	136.4	134.6	134.6	116.7	120.2	116.7
108	131.0	131.1	131.0	138.7	130.1	130.1	136.4	134.6	134.6	116.7	120.2	116.7
109	131.0	131.1	131.0	138.7	130.1	130.1	136.4	134.6	134.6	116.7	120.2	116.7
110	131.0	131.1	131.0	138.7	130.1	130.1	136.4	134.6	134.6	116.7	120.2	116.7
111	111.0	140.2	111.0	119.1	99.7	99.7	128.1	124.8	124.8	112.6	101.4	101.4
112	111.0	140.2	111.0	119.1	99.7	99.7	128.1	124.8	124.8	112.6	101.4	101.4
113	111.0	140.2	111.0	119.1	99.7	99.7	128.1	124.8	124.8	112.6	101.4	101.4
114	111.0	140.2	111.0	119.1	99.7	99.7	128.1	124.8	124.8	112.6	101.4	101.4
115	111.0	140.2	111.0	119.1	99.7	99.7	128.1	124.8	124.8	112.6	101.4	101.4
116	111.0	140.2	111.0	119.1	99.7	99.7	128.1	124.8	124.8	112.6	101.4	101.4
117	111.0	140.2	111.0	119.1	99.7	99.7	128.1	124.8	124.8	112.6	101.4	101.4
118	111.0	140.2	111.0	119.1	99.7	99.7	128.1	124.8	124.8	112.6	101.4	101.4
119	111.0	140.2	111.0	119.1	99.7	99.7	128.1	124.8	124.8	112.6	101.4	101.4
120	111.0	140.2	111.0	119.1	99.7	99.7	128.1	124.8	124.8	112.6	101.4	101.4
121	87.3	87.6	87.3	96.2	85.2	85.2	97.4	99.2	97.4	101.5	84.4	84.4
122	87.3	87.6	87.3	96.2	85.2	85.2	97.4	99.2	97.4	101.5	84.4	84.4
123	87.3	87.6	87.3	96.2	85.2	85.2	97.4	99.2	97.4	101.5	84.4	84.4
124	87.3	87.6	87.3	96.2	85.2	85.2	97.4	99.2	97.4	101.5	84.4	84.4
125	87.3	87.6	87.3	96.2	85.2	85.2	97.4	99.2	97.4	101.5	84.4	84.4
126	87.3	87.6	87.3	96.2	85.2	85.2	97.4	99.2	97.4	101.5	84.4	84.4

Table A-2 cont'd

	GNIA 0.1t	GNIA 0.1t	GNIA 0.1t	GNIA 0.2t	GNIA 0.2t	GNIA 0.2t	GNIA 0.5t	GNIA 0.5t	GNIA 0.5t	GNIA 1t	GNIA 1t	GNIA 1t
Analysis	**inward**	**outward**	**worst**	**inward**	**outward**	**worst**	**inward**	**outward**	**worst**	**inward**	**outward**	**worst**
Number	**MPa**	**MPa**	**MPa**	**MPa**	**MPa**	**MPa**	**MPa**	**MPa**	**MPa**	**MPa**	**MPa**	**MPa**
127	87.3	87.6	87.3	96.2	85.2	85.2	97.4	99.2	97.4	101.5	84.4	84.4
128	87.3	87.6	87.3	96.2	85.2	85.2	97.4	99.2	97.4	101.5	84.4	84.4
129	87.3	87.6	87.3	96.2	85.2	85.2	97.4	99.2	97.4	101.5	84.4	84.4
130	87.3	87.6	87.3	96.2	85.2	85.2	97.4	99.2	97.4	101.5	84.4	84.4
131	67.2	70.6	67.2	72.7	64.5	64.5	84.0	74.3	74.3	75.6	85.6	75.6
132	67.2	70.6	67.2	72.7	64.5	64.5	84.0	74.3	74.3	75.6	85.6	75.6
133	67.2	70.6	67.2	72.7	64.5	64.5	84.0	74.3	74.3	75.6	85.6	75.6
134	67.2	70.6	67.2	72.7	64.5	64.5	84.0	74.3	74.3	75.6	85.6	75.6
135	67.2	70.6	67.2	72.7	64.5	64.5	84.0	74.3	74.3	75.6	85.6	75.6
136	67.2	70.6	67.2	72.7	64.5	64.5	84.0	74.3	74.3	75.6	85.6	75.6
137	67.2	70.6	67.2	72.7	64.5	64.5	84.0	74.3	74.3	75.6	85.6	75.6
138	67.2	70.6	67.2	72.7	64.5	64.5	84.0	74.3	74.3	75.6	85.6	75.6
139	67.2	70.6	67.2	72.7	64.5	64.5	84.0	74.3	74.3	75.6	85.6	75.6
140	67.2	70.6	67.2	72.7	64.5	64.5	84.0	74.3	74.3	75.6	85.6	75.6
141	52.3	60.5	52.3	56.5	52.1	52.1	61.7	56.3	56.3	71.4	64.3	64.3
142	52.3	60.5	52.3	56.5	52.1	52.1	61.7	56.3	56.3	71.4	64.3	64.3
143	52.3	60.5	52.3	56.5	52.1	52.1	61.7	56.3	56.3	71.4	64.3	64.3
144	52.3	60.5	52.3	56.5	52.1	52.1	61.7	56.3	56.3	71.4	64.3	64.3
145	52.3	60.5	52.3	56.5	52.1	52.1	61.7	56.3	56.3	71.4	64.3	64.3
146	52.3	60.5	52.3	56.5	52.1	52.1	61.7	56.3	56.3	71.4	64.3	64.3
147	52.3	60.5	52.3	56.5	52.1	52.1	61.7	56.3	56.3	71.4	64.3	64.3

Table A-2 cont'd

	GNIA 0.1t	GNIA 0.1t	GNIA 0.1t	GNIA 0.2t	GNIA 0.2t	GNIA 0.2t	GNIA 0.5t	GNIA 0.5t	GNIA 0.5t	GNIA 1t	GNIA 1t	GNIA 1t
Analysis	**inward**	**outward**	**worst**	**inward**	**outward**	**worst**	**inward**	**outward**	**worst**	**inward**	**outward**	**worst**
Number	**MPa**	**MPa**	**MPa**	**MPa**	**MPa**	**MPa**	**MPa**	**MPa**	**MPa**	**MPa**	**MPa**	**MPa**
148	52.3	60.5	52.3	56.5	52.1	52.1	61.7	56.3	56.3	71.4	64.3	64.3
149	52.3	60.5	52.3	56.5	52.1	52.1	61.7	56.3	56.3	71.4	64.3	64.3
150	52.3	60.5	52.3	56.5	52.1	52.1	61.7	56.3	56.3	71.4	64.3	64.3
151	261.2	273.9	261.2	279.4	236.4	236.4	274.4	274.3	274.3	246.6	239.2	239.2
152	261.2	273.9	261.2	279.4	236.4	236.4	274.4	274.3	274.3	246.6	239.2	239.2
153	261.2	273.9	261.2	279.4	236.4	236.4	274.4	274.3	274.3	246.6	239.2	239.2
154	261.2	273.9	261.2	279.4	236.4	236.4	274.4	274.3	274.3	246.6	239.2	239.2
155	261.2	273.9	261.2	279.4	236.4	236.4	274.4	274.3	274.3	246.6	239.2	239.2
156	261.2	273.9	261.2	279.4	236.4	236.4	274.4	274.3	274.3	246.6	239.2	239.2
157	261.2	273.9	261.2	279.4	236.4	236.4	274.4	274.3	274.3	246.6	239.2	239.2
158	261.2	273.9	261.2	279.4	236.4	236.4	274.4	274.3	274.3	246.6	239.2	239.2
159	261.2	273.9	261.2	279.4	236.4	236.4	274.4	274.3	274.3	246.6	239.2	239.2
160	261.2	273.9	261.2	279.4	236.4	236.4	274.4	274.3	274.3	246.6	239.2	239.2
161	233.4	220.6	220.6	265.3	233.5	233.5	266.9	266.9	266.9	243.2	229.7	229.7
162	233.4	220.6	220.6	265.3	233.5	233.5	266.9	266.9	266.9	243.2	229.7	229.7
163	233.4	220.6	220.6	265.3	233.5	233.5	266.9	266.9	266.9	243.2	229.7	229.7
164	233.4	220.6	220.6	265.3	233.5	233.5	266.9	266.9	266.9	243.2	229.7	229.7
165	233.4	220.6	220.6	265.3	233.5	233.5	266.9	266.9	266.9	243.2	229.7	229.7
166	233.4	220.6	220.6	265.3	233.5	233.5	266.9	266.9	266.9	243.2	229.7	229.7
167	233.4	220.6	220.6	265.3	233.5	233.5	266.9	266.9	266.9	243.2	229.7	229.7
168	233.4	220.6	220.6	265.3	233.5	233.5	266.9	266.9	266.9	243.2	229.7	229.7

Table A-2 cont'd

	GNIA 0.1t	GNIA 0.1t	GNIA 0.1t	GNIA 0.2t	GNIA 0.2t	GNIA 0.2t	GNIA 0.5t	GNIA 0.5t	GNIA 0.5t	GNIA 1t	GNIA 1t	GNIA 1t
Analysis	**inward**	**outward**	**worst**	**inward**	**outward**	**worst**	**inward**	**outward**	**worst**	**inward**	**outward**	**worst**
Number	**MPa**	**MPa**	**MPa**	**MPa**	**MPa**	**MPa**	**MPa**	**MPa**	**MPa**	**MPa**	**MPa**	**MPa**
169	233.4	220.6	220.6	265.3	233.5	233.5	266.9	266.9	266.9	243.2	229.7	229.7
170	233.4	220.6	220.6	265.3	233.5	233.5	266.9	266.9	266.9	243.2	229.7	229.7
171	177.4	183.7	177.4	194.1	169.8	169.8	223.8	193.5	193.5	196.1	222.1	196.1
172	177.4	183.7	177.4	194.1	169.8	169.8	223.8	193.5	193.5	196.1	222.1	196.1
173	177.4	183.7	177.4	194.1	169.8	169.8	223.8	193.5	193.5	196.1	222.1	196.1
174	177.4	183.7	177.4	194.1	169.8	169.8	223.8	193.5	193.5	196.1	222.1	196.1
175	177.4	183.7	177.4	194.1	169.8	169.8	223.8	193.5	193.5	196.1	222.1	196.1
176	177.4	183.7	177.4	194.1	169.8	169.8	223.8	193.5	193.5	196.1	222.1	196.1
177	177.4	183.7	177.4	194.1	169.8	169.8	223.8	193.5	193.5	196.1	222.1	196.1
178	177.4	183.7	177.4	194.1	169.8	169.8	223.8	193.5	193.5	196.1	222.1	196.1
179	177.4	183.7	177.4	194.1	169.8	169.8	223.8	193.5	193.5	196.1	222.1	196.1
180	177.4	183.7	177.4	194.1	169.8	169.8	223.8	193.5	193.5	196.1	222.1	196.1
181	141.6	153.7	141.6	149.4	136.2	136.2	171.4	145.5	145.5	191.3	165.1	165.1
182	141.6	153.7	141.6	149.4	136.2	136.2	171.4	145.5	145.5	191.3	165.1	165.1
183	141.6	153.7	141.6	149.4	136.2	136.2	171.4	145.5	145.5	191.3	165.1	165.1
184	141.6	153.7	141.6	149.4	136.2	136.2	171.4	145.5	145.5	191.3	165.1	165.1
185	141.6	153.7	141.6	149.4	136.2	136.2	171.4	145.5	145.5	191.3	165.1	165.1
186	141.6	153.7	141.6	149.4	136.2	136.2	171.4	145.5	145.5	191.3	165.1	165.1
187	141.6	153.7	141.6	149.4	136.2	136.2	171.4	145.5	145.5	191.3	165.1	165.1
188	141.6	153.7	141.6	149.4	136.2	136.2	171.4	145.5	145.5	191.3	165.1	165.1
189	141.6	153.7	141.6	149.4	136.2	136.2	171.4	145.5	145.5	191.3	165.1	165.1

Table A-2 cont'd

	GNIA 0.1t	GNIA 0.1t	GNIA 0.1t	GNIA 0.2t	GNIA 0.2t	GNIA 0.2t	GNIA 0.5t	GNIA 0.5t	GNIA 0.5t	GNIA 1t	GNIA 1t	GNIA 1t
Analysis	**inward**	**outward**	**worst**	**inward**	**outward**	**worst**	**inward**	**outward**	**worst**	**inward**	**outward**	**worst**
Number	**MPa**	**MPa**	**MPa**	**MPa**	**MPa**	**MPa**	**MPa**	**MPa**	**MPa**	**MPa**	**MPa**	**MPa**
190	141.6	153.7	141.6	149.4	136.2	136.2	171.4	145.5	145.5	191.3	165.1	165.1
191	117.1	130.0	117.1	117.9	107.7	107.7	131.7	112.9	112.9	148.4	125.3	125.3
192	117.1	130.0	117.1	117.9	107.7	107.7	131.7	112.9	112.9	148.4	125.3	125.3
193	117.1	130.0	117.1	117.9	107.7	107.7	131.7	112.9	112.9	148.4	125.3	125.3
194	117.1	130.0	117.1	117.9	107.7	107.7	131.7	112.9	112.9	148.4	125.3	125.3
195	117.1	130.0	117.1	117.9	107.7	107.7	131.7	112.9	112.9	148.4	125.3	125.3
196	117.1	130.0	117.1	117.9	107.7	107.7	131.7	112.9	112.9	148.4	125.3	125.3
197	117.1	130.0	117.1	117.9	107.7	107.7	131.7	112.9	112.9	148.4	125.3	125.3
198	117.1	130.0	117.1	117.9	107.7	107.7	131.7	112.9	112.9	148.4	125.3	125.3
199	117.1	130.0	117.1	117.9	107.7	107.7	131.7	112.9	112.9	148.4	125.3	125.3
200	117.1	130.0	117.1	117.9	107.7	107.7	131.7	112.9	112.9	148.4	125.3	125.3

Table A-3: GNIA Results for 2t and 3t Imperfection Cases, GMNA Results and GMNIA Results for 3t and 0.2t Imperfection Cases

	GNIA 2t	GNIA 2t	GNIA 2t	GNIA 3t	GNIA 3t	GNIA 3t	GMNA	GMNIA 3t	GMNIA 3t	GMNIA 3t	GMNIA 0.2t	GMNIA 0.2t	GMNIA 0.2t
Analysis	**inward**	**outward**	**worst**	**inward**	**outward**	**worst**		**inward**	**outward**	**worst**	**inward**	**outward**	**worst**
Number	**MPa**	**MPa**	**MPa**	**MPa**	**MPa**	**MPa**	**MPa**	**MPa**	**MPa**	**MPa**	**MPa**	**MPa**	**MPa**
1	56.2	55.8	55.8	56.2	51.9	51.9	1.0	0.9	0.9	0.9	1.0	1.0	1.0
2	56.2	55.8	55.8	56.2	51.9	51.9	9.8	8.4	8.4	8.4	9.7	9.6	9.6
3	56.2	55.8	55.8	56.2	51.9	51.9	22.3	19.6	19.7	19.6	21.8	21.8	21.8
4	56.2	55.8	55.8	56.2	51.9	51.9	40.8	33.8	34.3	33.8	35.2	35.5	35.2
5	56.2	55.8	55.8	56.2	51.9	51.9	59.0	41.6	43.4	41.6	44.3	47.0	44.3
6	56.2	55.8	55.8	56.2	51.9	51.9	75.6	47.4	49.2	47.4	50.0	51.1	50.0
7	56.2	55.8	55.8	56.2	51.9	51.9	99.5	53.5	50.4	50.4	54.6	55.6	54.6
8	56.2	55.8	55.8	56.2	51.9	51.9	97.6	55.7	51.7	51.7	63.9	55.6	55.6
9	56.2	55.8	55.8	56.2	51.9	51.9	97.6	56.1	51.9	51.9	54.8	55.6	54.8
10	56.2	55.8	55.8	56.2	51.9	51.9	97.6	56.1	51.9	51.9	54.8	55.6	54.8
11	44.9	47.4	44.9	44.6	43.6	43.6	1.0	0.9	0.9	0.9	1.0	1.0	1.0
12	44.9	47.4	44.9	44.6	43.6	43.6	9.4	8.5	8.4	8.4	9.2	9.3	9.2
13	44.9	47.4	44.9	44.6	43.6	43.6	20.0	18.7	18.7	18.7	19.4	19.5	19.4
14	44.9	47.4	44.9	44.6	43.6	43.6	34.9	30.9	30.6	30.6	30.5	30.2	30.2
15	44.9	47.4	44.9	44.6	43.6	43.6	50.9	34.3	35.8	34.3	38.5	38.3	38.3
16	44.9	47.4	44.9	44.6	43.6	43.6	66.2	39.6	41.9	39.6	44.1	42.9	42.9
17	44.9	47.4	44.9	44.6	43.6	43.6	83.3	43.1	42.8	42.8	52.7	46.4	46.4
18	44.9	47.4	44.9	44.6	43.6	43.6	83.6	44.4	43.6	43.6	56.0	54.8	54.8
19	44.9	47.4	44.9	44.6	43.6	43.6	83.6	44.6	43.6	43.6	58.0	54.5	54.5
20	44.9	47.4	44.9	44.6	43.6	43.6	83.6	44.6	43.6	43.6	58.1	55.3	55.3

Table A-3 cont'd

	GNIA 2t	GNIA 2t	GNIA 2t	GNIA 3t	GNIA 3t	GNIA 3t	GMNA	GMNIA 3t	GMNIA 3t	GMNIA 3t	GMNIA 0.2t	GMNIA 0.2t	GMNIA 0.2t
Analysis	**inward**	**outward**	**worst**	**inward**	**outward**	**worst**		**inward**	**outward**	**worst**	**inward**	**outward**	**worst**
Number	**MPa**	**MPa**	**MPa**	**MPa**	**MPa**	**MPa**	**MPa**	**MPa**	**MPa**	**MPa**	**MPa**	**MPa**	**MPa**
21	34.5	35.0	34.5	34.1	34.2	34.1	1.0	0.9	0.9	0.9	1.0	1.0	1.0
22	34.5	35.0	34.5	34.1	34.2	34.1	8.2	8.0	8.0	8.0	8.2	8.2	8.2
23	34.5	35.0	34.5	34.1	34.2	34.1	16.1	15.2	15.8	15.2	15.7	15.8	15.7
24	34.5	35.0	34.5	34.1	34.2	34.1	26.7	21.3	25.1	21.3	25.6	23.3	23.3
25	34.5	35.0	34.5	34.1	34.2	34.1	38.7	25.8	32.2	25.8	33.7	28.6	28.6
26	34.5	35.0	34.5	34.1	34.2	34.1	50.2	30.0	37.8	30.0	39.3	33.5	33.5
27	34.5	35.0	34.5	34.1	34.2	34.1	62.4	33.8	34.2	33.8	42.7	39.5	39.5
28	34.5	35.0	34.5	34.1	34.2	34.1	63.1	34.0	34.2	34.0	46.6	41.6	41.6
29	34.5	35.0	34.5	34.1	34.2	34.1	63.1	34.1	43.6	34.1	46.9	43.1	43.1
30	34.5	35.0	34.5	34.1	34.2	34.1	63.1	34.1	34.2	34.1	47.7	43.2	43.2
31	29.7	32.9	29.7	26.8	27.7	26.8	1.0	0.9	0.9	0.9	1.0	1.0	1.0
32	29.7	32.9	29.7	26.8	27.7	26.8	7.0	7.0	7.0	7.0	7.0	7.1	7.0
33	29.7	32.9	29.7	26.8	27.7	26.8	13.3	11.9	13.4	11.9	13.4	13.2	13.2
34	29.7	32.9	29.7	26.8	27.7	26.8	21.8	17.9	20.4	17.9	19.2	18.5	18.5
35	29.7	32.9	29.7	26.8	27.7	26.8	31.6	22.7	21.6	21.6	24.2	23.0	23.0
36	29.7	32.9	29.7	26.8	27.7	26.8	40.7	25.1	32.7	25.1	27.4	26.5	26.5
37	29.7	32.9	29.7	26.8	27.7	26.8	48.7	26.0	30.2	26.0	33.5	32.1	32.1
38	29.7	32.9	29.7	26.8	27.7	26.8	49.0	26.5	28.0	26.5	35.6	32.4	32.4
39	29.7	32.9	29.7	26.8	27.7	26.8	49.0	26.8	27.7	26.8	28.7	31.9	28.7
40	29.7	32.9	29.7	26.8	27.7	26.8	49.0	26.8	27.7	26.8	28.7	32.2	28.7
41	25.7	26.1	25.7	25.4	26.7	25.4	1.0	0.9	0.9	0.9	0.9	0.9	0.9

Table A-3 cont'd

	GNIA 2t	GNIA 2t	GNIA 2t	GNIA 3t	GNIA 3t	GNIA 3t	GMNA	GMNIA 3t	GMNIA 3t	GMNIA 3t	GMNIA 0.2t	GMNIA 0.2t	GMNIA 0.2t
Analysis	**inward**	**outward**	**worst**	**inward**	**outward**	**worst**		**inward**	**outward**	**worst**	**inward**	**outward**	**worst**
Number	**MPa**	**MPa**	**MPa**	**MPa**	**MPa**	**MPa**	**MPa**	**MPa**	**MPa**	**MPa**	**MPa**	**MPa**	**MPa**
42	25.7	26.1	25.7	25.4	26.7	25.4	5.9	6.1	6.0	6.0	5.9	6.0	5.9
43	25.7	26.1	25.7	25.4	26.7	25.4	11.1	11.3	11.6	11.3	11.4	10.3	10.3
44	25.7	26.1	25.7	25.4	26.7	25.4	18.3	15.9	14.7	14.7	15.9	15.7	15.7
45	25.7	26.1	25.7	25.4	26.7	25.4	26.2	20.7	18.1	18.1	19.6	19.6	19.6
46	25.7	26.1	25.7	25.4	26.7	25.4	33.3	23.9	21.4	21.4	22.4	21.8	21.8
47	25.7	26.1	25.7	25.4	26.7	25.4	38.4	24.9	23.8	23.8	27.5	26.4	26.4
48	25.7	26.1	25.7	25.4	26.7	25.4	38.2	25.4	26.3	25.4	27.0	24.3	24.3
49	25.7	26.1	25.7	25.4	26.7	25.4	38.2	25.4	26.7	25.4	27.3	24.2	24.2
50	25.7	26.1	25.7	25.4	26.7	25.4	41.0	25.4	26.8	25.4	27.4	24.2	24.2
51	73.3	69.4	69.4	68.6	67.7	67.7	1.0	0.9	0.9	0.9	1.0	1.0	1.0
52	73.3	69.4	69.4	68.6	67.7	67.7	9.9	8.3	8.3	8.3	9.7	9.8	9.7
53	73.3	69.4	69.4	68.6	67.7	67.7	23.5	20.1	20.1	20.1	23.0	23.0	23.0
54	73.3	69.4	69.4	68.6	67.7	67.7	42.5	36.7	36.8	36.7	40.8	39.8	39.8
55	73.3	69.4	69.4	68.6	67.7	67.7	60.9	47.9	47.2	47.2	57.2	51.3	51.3
56	73.3	69.4	69.4	68.6	67.7	67.7	79.2	55.6	53.8	53.8	61.6	59.9	59.9
57	73.3	69.4	69.4	68.6	67.7	67.7	111.0	66.2	62.4	62.4	82.0	69.0	69.0
58	73.3	69.4	69.4	68.6	67.7	67.7	129.0	66.8	66.0	66.0	91.5	73.2	73.2
59	73.3	69.4	69.4	68.6	67.7	67.7	131.1	68.1	62.4	62.4	74.2	88.4	74.2
60	73.3	69.4	69.4	68.6	67.7	67.7	131.1	68.1	67.4	67.4	74.2	87.5	74.2
61	62.4	63.7	62.4	59.9	64.3	59.9	1.0	0.9	0.9	0.9	1.0	1.0	1.0
62	62.4	63.7	62.4	59.9	64.3	59.9	9.7	8.6	8.5	8.5	9.6	9.6	9.6

Table A-3 cont'd

	GNIA 2t	GNIA 2t	GNIA 2t	GNIA 3t	GNIA 3t	GNIA 3t	GMNA	GMNIA 3t	GMNIA 3t	GMNIA 3t	GMNIA 0.2t	GMNIA 0.2t	GMNIA 0.2t
Analysis	**inward**	**outward**	**worst**	**inward**	**outward**	**worst**		**inward**	**outward**	**worst**	**inward**	**outward**	**worst**
Number	**MPa**	**MPa**	**MPa**	**MPa**	**MPa**	**MPa**	**MPa**	**MPa**	**MPa**	**MPa**	**MPa**	**MPa**	**MPa**
63	62.4	63.7	62.4	59.9	64.3	59.9	21.6	19.9	19.8	19.8	21.2	21.2	21.2
64	62.4	63.7	62.4	59.9	64.3	59.9	36.9	34.4	32.1	32.1	35.2	34.5	34.5
65	62.4	63.7	62.4	59.9	64.3	59.9	52.3	45.3	40.3	40.3	44.5	44.9	44.5
66	62.4	63.7	62.4	59.9	64.3	59.9	67.9	48.1	47.0	47.0	52.0	60.2	52.0
67	62.4	63.7	62.4	59.9	64.3	59.9	97.4	55.7	55.6	55.6	64.4	61.9	61.9
68	62.4	63.7	62.4	59.9	64.3	59.9	110.3	58.3	60.4	58.3	71.3	71.7	71.3
69	62.4	63.7	62.4	59.9	64.3	59.9	113.7	59.9	64.3	59.9	77.1	71.4	71.4
70	62.4	63.7	62.4	59.9	64.3	59.9	112.9	59.9	64.3	59.9	79.1	74.0	74.0
71	46.7	54.1	46.7	45.7	48.1	45.7	1.0	0.9	0.9	0.9	1.0	1.0	1.0
72	46.7	54.1	46.7	45.7	48.1	45.7	8.9	8.4	8.3	8.3	8.8	8.7	8.7
73	46.7	54.1	46.7	45.7	48.1	45.7	18.0	16.9	17.1	16.9	17.8	18.1	17.8
74	46.7	54.1	46.7	45.7	48.1	45.7	28.7	25.5	28.3	25.5	28.8	25.9	25.9
75	46.7	54.1	46.7	45.7	48.1	45.7	40.3	32.0	37.2	32.0	35.1	33.9	33.9
76	46.7	54.1	46.7	45.7	48.1	45.7	52.3	37.5	44.3	37.5	40.8	39.3	39.3
77	46.7	54.1	46.7	45.7	48.1	45.7	74.1	43.9	59.0	43.9	51.2	48.3	48.3
78	46.7	54.1	46.7	45.7	48.1	45.7	83.7	45.4	53.8	45.4	57.1	53.1	53.1
79	46.7	54.1	46.7	45.7	48.1	45.7	82.7	45.7	47.6	45.7	62.7	56.7	56.7
80	46.7	54.1	46.7	45.7	48.1	45.7	82.7	45.7	48.1	45.7	48.5	57.2	48.5
81	43.5	40.8	40.8	37.6	40.7	37.6	1.0	0.9	0.9	0.9	1.0	1.0	1.0
82	43.5	40.8	40.8	37.6	40.7	37.6	7.8	7.7	7.6	7.6	7.8	7.8	7.8
83	43.5	40.8	40.8	37.6	40.7	37.6	15.3	15.2	14.9	14.9	15.2	15.3	15.2

Table A-3 cont'd

	GNIA 2t	GNIA 2t	GNIA 2t	GNIA 3t	GNIA 3t	GNIA 3t	GMNA	GMNIA 3t	GMNIA 3t	GMNIA 3t	GMNIA 0.2t	GMNIA 0.2t	GMNIA 0.2t
Analysis	**inward**	**outward**	**worst**	**inward**	**outward**	**worst**		**inward**	**outward**	**worst**	**inward**	**outward**	**worst**
Number	**MPa**	**MPa**	**MPa**	**MPa**	**MPa**	**MPa**	**MPa**	**MPa**	**MPa**	**MPa**	**MPa**	**MPa**	**MPa**
84	43.5	40.8	40.8	37.6	40.7	37.6	23.2	22.3	23.8	22.3	23.0	21.2	21.2
85	43.5	40.8	40.8	37.6	40.7	37.6	32.9	28.4	30.7	28.4	27.6	26.8	26.8
86	43.5	40.8	40.8	37.6	40.7	37.6	42.5	34.6	30.8	30.8	32.8	31.6	31.6
87	43.5	40.8	40.8	37.6	40.7	37.6	58.7	38.0	35.9	35.9	38.3	37.0	37.0
88	43.5	40.8	40.8	37.6	40.7	37.6	64.9	40.0	37.6	37.6	45.7	44.1	44.1
89	43.5	40.8	40.8	37.6	40.7	37.6	64.5	37.6	40.6	37.6	47.4	42.6	42.6
90	43.5	40.8	40.8	37.6	40.7	37.6	64.5	37.6	40.6	37.6	48.2	42.7	42.7
91	34.3	34.5	34.3	44.8	34.5	34.5	1.0	0.9	0.9	0.9	1.0	1.0	1.0
92	34.3	34.5	34.3	44.8	34.5	34.5	6.7	6.7	6.7	6.7	6.7	6.7	6.7
93	34.3	34.5	34.3	44.8	34.5	34.5	12.6	12.9	12.9	12.9	12.9	13.0	12.9
94	34.3	34.5	34.3	44.8	34.5	34.5	19.3	17.5	20.0	17.5	18.9	17.9	17.9
95	34.3	34.5	34.3	44.8	34.5	34.5	27.5	24.2	25.6	24.2	23.1	23.7	23.1
96	34.3	34.5	34.3	44.8	34.5	34.5	35.5	29.3	33.2	29.3	26.4	26.9	26.4
97	34.3	34.5	34.3	44.8	34.5	34.5	47.6	33.4	30.6	30.6	33.2	30.8	30.8
98	34.3	34.5	34.3	44.8	34.5	34.5	50.9	37.6	33.0	33.0	37.0	31.2	31.2
99	34.3	34.5	34.3	44.8	34.5	34.5	51.6	41.5	34.4	34.4	36.5	32.5	32.5
100	34.3	34.5	34.3	44.8	34.5	34.5	51.6	44.3	34.5	34.5	35.8	32.6	32.6
101	107.5	108.4	107.5	106.8	101.3	101.3	0.8	0.8	0.8	0.8	1.0	1.0	1.0
102	107.5	108.4	107.5	106.8	101.3	101.3	8.2	8.2	8.2	8.2	9.8	9.8	9.8
103	107.5	108.4	107.5	106.8	101.3	101.3	20.1	20.2	20.2	20.2	24.0	24.0	24.0
104	107.5	108.4	107.5	106.8	101.3	101.3	38.5	38.7	38.7	38.7	44.8	44.5	44.5

Table A-3 cont'd

	GNIA 2t	GNIA 2t	GNIA 2t	GNIA 3t	GNIA 3t	GNIA 3t	GMNA	GMNIA 3t	GMNIA 3t	GMNIA 3t	GMNIA 0.2t	GMNIA 0.2t	GMNIA 0.2t
Analysis	**inward**	**outward**	**worst**	**inward**	**outward**	**worst**		**inward**	**outward**	**worst**	**inward**	**outward**	**worst**
Number	**MPa**	**MPa**	**MPa**	**MPa**	**MPa**	**MPa**	**MPa**	**MPa**	**MPa**	**MPa**	**MPa**	**MPa**	**MPa**
105	107.5	108.4	107.5	106.8	101.3	101.3	54.4	54.9	54.9	54.9	62.4	61.8	61.8
106	107.5	108.4	107.5	106.8	101.3	101.3	66.9	68.4	68.4	68.4	73.9	73.3	73.3
107	107.5	108.4	107.5	106.8	101.3	101.3	82.7	89.6	89.6	89.6	92.4	92.0	92.0
108	107.5	108.4	107.5	106.8	101.3	101.3	93.3	92.9	92.9	92.9	104.5	101.8	101.8
109	107.5	108.4	107.5	106.8	101.3	101.3	103.6	99.6	99.6	99.6	128.7	111.8	111.8
110	107.5	108.4	107.5	106.8	101.3	101.3	106.6	101.0	101.0	101.0	139.6	130.1	130.1
111	100.5	108.4	100.5	96.1	94.9	94.9	0.9	0.9	0.9	0.9	1.0	1.0	1.0
112	100.5	108.4	100.5	96.1	94.9	94.9	8.4	8.4	8.4	8.4	9.8	9.7	9.7
113	100.5	108.4	100.5	96.1	94.9	94.9	20.5	20.4	20.4	20.4	23.2	23.1	23.1
114	100.5	108.4	100.5	96.1	94.9	94.9	37.8	36.7	36.7	36.7	41.1	41.2	41.1
115	100.5	108.4	100.5	96.1	94.9	94.9	51.4	48.5	48.5	48.5	54.5	56.1	54.5
116	100.5	108.4	100.5	96.1	94.9	94.9	63.0	57.5	57.5	57.5	62.5	67.3	62.5
117	100.5	108.4	100.5	96.1	94.9	94.9	82.9	73.0	73.0	73.0	78.4	92.5	78.4
118	100.5	108.4	100.5	96.1	94.9	94.9	85.8	82.4	82.4	82.4	88.6	107.5	88.6
119	100.5	108.4	100.5	96.1	94.9	94.9	93.4	91.3	91.3	91.3	111.0	117.5	111.0
120	100.5	108.4	100.5	96.1	94.9	94.9	95.0	94.9	94.9	94.9	118.8	99.7	99.7
121	83.6	77.6	77.6	75.1	77.2	75.1	0.9	0.9	0.9	0.9	1.0	1.0	1.0
122	83.6	77.6	77.6	75.1	77.2	75.1	8.5	8.5	8.5	8.5	9.4	9.4	9.4
123	83.6	77.6	77.6	75.1	77.2	75.1	19.4	19.1	19.1	19.1	20.6	20.7	20.6
124	83.6	77.6	77.6	75.1	77.2	75.1	33.7	31.3	31.3	31.3	33.6	34.4	33.6
125	83.6	77.6	77.6	75.1	77.2	75.1	44.2	39.8	39.8	39.8	45.0	40.3	40.3

Table A-3 cont'd

	GNIA 2t	GNIA 2t	GNIA 2t	GNIA 3t	GNIA 3t	GNIA 3t	GMNA	GMNIA 3t	GMNIA 3t	GMNIA 3t	GMNIA 0.2t	GMNIA 0.2t	GMNIA 0.2t
Analysis	**inward**	**outward**	**worst**	**inward**	**outward**	**worst**		**inward**	**outward**	**worst**	**inward**	**outward**	**worst**
Number	**MPa**	**MPa**	**MPa**	**MPa**	**MPa**	**MPa**	**MPa**	**MPa**	**MPa**	**MPa**	**MPa**	**MPa**	**MPa**
126	83.6	77.6	77.6	75.1	77.2	75.1	51.7	48.3	48.3	48.3	49.3	48.7	48.7
127	83.6	77.6	77.6	75.1	77.2	75.1	64.9	58.4	58.4	58.4	62.6	61.5	61.5
128	83.6	77.6	77.6	75.1	77.2	75.1	67.0	66.7	66.7	66.7	80.5	68.8	68.8
129	83.6	77.6	77.6	75.1	77.2	75.1	73.2	73.9	73.9	73.9	91.0	86.4	86.4
130	83.6	77.6	77.6	75.1	77.2	75.1	74.7	77.2	77.2	77.2	96.0	85.3	85.3
131	83.1	67.6	67.6	71.5	63.5	63.5	0.9	0.9	0.9	0.9	1.0	1.0	1.0
132	83.1	67.6	67.6	71.5	63.5	63.5	8.2	8.2	8.2	8.2	8.7	8.7	8.7
133	83.1	67.6	67.6	71.5	63.5	63.5	17.6	17.0	17.0	17.0	17.9	18.0	17.9
134	83.1	67.6	67.6	71.5	63.5	63.5	28.4	27.0	27.0	27.0	29.5	29.2	29.2
135	83.1	67.6	67.6	71.5	63.5	63.5	36.0	37.4	37.4	37.4	37.5	33.6	33.6
136	83.1	67.6	67.6	71.5	63.5	63.5	40.2	48.9	48.9	48.9	39.5	41.1	39.5
137	83.1	67.6	67.6	71.5	63.5	63.5	50.4	49.4	49.4	49.4	58.1	47.5	47.5
138	83.1	67.6	67.6	71.5	63.5	63.5	58.2	55.1	55.1	55.1	56.2	56.1	56.1
139	83.1	67.6	67.6	71.5	63.5	63.5	74.5	61.9	61.9	61.9	72.6	70.7	70.7
140	83.1	67.6	67.6	71.5	63.5	63.5	71.5	63.5	63.5	63.5	72.7	64.5	64.5
141	62.8	80.7	62.8	68.4	52.1	52.1	0.9	0.9	0.9	0.9	1.0	1.0	1.0
142	62.8	80.7	62.8	68.4	52.1	52.1	7.6	7.7	7.7	7.7	7.8	7.9	7.8
143	62.8	80.7	62.8	68.4	52.1	52.1	15.3	14.9	14.9	14.9	15.5	15.5	15.5
144	62.8	80.7	62.8	68.4	52.1	52.1	23.8	24.5	24.5	24.5	24.9	24.4	24.4
145	62.8	80.7	62.8	68.4	52.1	52.1	30.3	32.2	32.2	32.2	26.9	30.1	26.9
146	62.8	80.7	62.8	68.4	52.1	52.1	32.7	38.4	38.4	38.4	39.9	35.5	35.5

Table A-3 cont'd

	GNIA 2t	GNIA 2t	GNIA 2t	GNIA 3t	GNIA 3t	GNIA 3t	GMNA	GMNIA 3t	GMNIA 3t	GMNIA 3t	GMNIA 0.2t	GMNIA 0.2t	GMNIA 0.2t
Analysis	**inward**	**outward**	**worst**	**inward**	**outward**	**worst**		**inward**	**outward**	**worst**	**inward**	**outward**	**worst**
Number	**MPa**	**MPa**	**MPa**	**MPa**	**MPa**	**MPa**	**MPa**	**MPa**	**MPa**	**MPa**	**MPa**	**MPa**	**MPa**
147	62.8	80.7	62.8	68.4	52.1	52.1	41.2	43.3	43.3	43.3	40.1	43.9	40.1
148	62.8	80.7	62.8	68.4	52.1	52.1	47.2	50.4	50.4	50.4	46.0	49.3	46.0
149	62.8	80.7	62.8	68.4	52.1	52.1	56.2	58.4	58.4	58.4	59.1	52.1	52.1
150	62.8	80.7	62.8	68.4	52.1	52.1	68.2	52.1	52.1	52.1	56.4	52.1	52.1
151	217.8	221.9	217.8	207.3	219.6	207.3	0.8	0.8	0.8	0.8	1.0	1.0	1.0
152	217.8	221.9	217.8	207.3	219.6	207.3	7.8	7.8	7.8	7.8	9.8	9.8	9.8
153	217.8	221.9	217.8	207.3	219.6	207.3	19.2	19.1	19.1	19.1	24.4	24.4	24.4
154	217.8	221.9	217.8	207.3	219.6	207.3	37.6	37.6	37.6	37.6	47.9	48.1	47.9
155	217.8	221.9	217.8	207.3	219.6	207.3	55.3	55.6	55.6	55.6	70.2	70.6	70.2
156	217.8	221.9	217.8	207.3	219.6	207.3	72.4	73.0	73.0	73.0	91.0	91.8	91.0
157	217.8	221.9	217.8	207.3	219.6	207.3	103.7	104.0	104.0	104.0	126.6	127.3	126.6
158	217.8	221.9	217.8	207.3	219.6	207.3	131.7	130.8	130.8	130.8	150.6	153.3	150.6
159	217.8	221.9	217.8	207.3	219.6	207.3	164.7	167.8	167.8	167.8	189.5	193.3	189.5
160	217.8	221.9	217.8	207.3	219.6	207.3	204.2	219.5	219.5	219.5	260.2	234.6	234.6
161	202.8	213.0	202.8	195.3	216.6	195.3	0.8	0.8	0.8	0.8	1.0	1.0	1.0
162	202.8	213.0	202.8	195.3	216.6	195.3	8.1	8.1	8.1	8.1	9.8	9.8	9.8
163	202.8	213.0	202.8	195.3	216.6	195.3	20.1	20.0	20.0	20.0	24.2	24.2	24.2
164	202.8	213.0	202.8	195.3	216.6	195.3	39.6	39.1	39.1	39.1	46.8	47.1	46.8
165	202.8	213.0	202.8	195.3	216.6	195.3	58.3	57.4	57.4	57.4	67.4	67.8	67.4
166	202.8	213.0	202.8	195.3	216.6	195.3	75.7	74.6	74.6	74.6	85.5	85.7	85.5
167	202.8	213.0	202.8	195.3	216.6	195.3	103.8	104.3	104.3	104.3	115.2	111.6	111.6

Table A-3 cont'd

	GNIA 2t	GNIA 2t	GNIA 2t	GNIA 3t	GNIA 3t	GNIA 3t	GMNA	GMNIA 3t	GMNIA 3t	GMNIA 3t	GMNIA 0.2t	GMNIA 0.2t	GMNIA 0.2t
Analysis	**inward**	**outward**	**worst**	**inward**	**outward**	**worst**		**inward**	**outward**	**worst**	**inward**	**outward**	**worst**
Number	**MPa**	**MPa**	**MPa**	**MPa**	**MPa**	**MPa**	**MPa**	**MPa**	**MPa**	**MPa**	**MPa**	**MPa**	**MPa**
168	202.8	213.0	202.8	195.3	216.6	195.3	127.6	128.8	128.8	128.8	138.6	130.1	130.1
169	202.8	213.0	202.8	195.3	216.6	195.3	157.7	161.9	161.9	161.9	174.0	165.1	165.1
170	202.8	213.0	202.8	195.3	216.6	195.3	192.9	222.2	222.2	222.2	243.2	230.6	230.6
171	200.5	176.2	176.2	189.5	168.0	168.0	0.8	0.8	0.8	0.8	1.0	1.0	1.0
172	200.5	176.2	176.2	189.5	168.0	168.0	8.3	8.4	8.4	8.4	9.8	9.8	9.8
173	200.5	176.2	176.2	189.5	168.0	168.0	20.3	20.5	20.5	20.5	23.7	23.6	23.6
174	200.5	176.2	176.2	189.5	168.0	168.0	38.7	39.2	39.2	39.2	43.6	43.2	43.2
175	200.5	176.2	176.2	189.5	168.0	168.0	54.7	54.9	54.9	54.9	59.9	60.2	59.9
176	200.5	176.2	176.2	189.5	168.0	168.0	68.0	68.4	68.4	68.4	74.0	75.1	74.0
177	200.5	176.2	176.2	189.5	168.0	168.0	90.5	91.8	91.8	91.8	96.8	91.2	91.2
178	200.5	176.2	176.2	189.5	168.0	168.0	108.2	109.3	109.3	109.3	113.4	108.4	108.4
179	200.5	176.2	176.2	189.5	168.0	168.0	137.1	138.4	138.4	138.4	130.9	130.5	130.5
180	200.5	176.2	176.2	189.5	168.0	168.0	184.1	165.3	165.3	165.3	191.7	159.3	159.3
181	153.2	195.7	153.2	159.0	155.8	155.8	0.9	0.9	0.9	0.9	1.0	1.0	1.0
182	153.2	195.7	153.2	159.0	155.8	155.8	8.3	8.4	8.4	8.4	9.6	9.6	9.6
183	153.2	195.7	153.2	159.0	155.8	155.8	19.9	20.3	20.3	20.3	22.1	22.2	22.1
184	153.2	195.7	153.2	159.0	155.8	155.8	36.3	37.2	37.2	37.2	39.0	39.1	39.0
185	153.2	195.7	153.2	159.0	155.8	155.8	49.2	50.0	50.0	50.0	52.6	52.7	52.6
186	153.2	195.7	153.2	159.0	155.8	155.8	59.5	60.5	60.5	60.5	64.2	64.3	64.2
187	153.2	195.7	153.2	159.0	155.8	155.8	76.9	78.6	78.6	78.6	82.3	81.3	81.3
188	153.2	195.7	153.2	159.0	155.8	155.8	91.2	93.6	93.6	93.6	84.8	93.5	84.8

Table A-3 cont'd

	GNIA 2t	GNIA 2t	GNIA 2t	GNIA 3t	GNIA 3t	GNIA 3t	GMNA	GMNIA 3t	GMNIA 3t	GMNIA 3t	GMNIA 0.2t	GMNIA 0.2t	GMNIA 0.2t
Analysis	**inward**	**outward**	**worst**	**inward**	**outward**	**worst**		**inward**	**outward**	**worst**	**inward**	**outward**	**worst**
Number	**MPa**	**MPa**	**MPa**	**MPa**	**MPa**	**MPa**	**MPa**	**MPa**	**MPa**	**MPa**	**MPa**	**MPa**	**MPa**
189	153.2	195.7	153.2	159.0	155.8	155.8	111.5	115.8	115.8	115.8	105.2	108.9	105.2
190	153.2	195.7	153.2	159.0	155.8	155.8	143.7	164.7	164.7	164.7	156.9	133.1	133.1
191	130.1	143.8	130.1	132.5	160.0	132.5	0.9	0.9	0.9	0.9	1.0	1.0	1.0
192	130.1	143.8	130.1	132.5	160.0	132.5	8.2	8.3	8.3	8.3	9.3	9.3	9.3
193	130.1	143.8	130.1	132.5	160.0	132.5	18.7	18.8	18.8	18.8	20.1	20.3	20.1
194	130.1	143.8	130.1	132.5	160.0	132.5	32.3	31.3	31.3	31.3	34.1	33.9	33.9
195	130.1	143.8	130.1	132.5	160.0	132.5	42.8	43.8	43.8	43.8	45.4	44.5	44.5
196	130.1	143.8	130.1	132.5	160.0	132.5	51.2	52.9	52.9	52.9	54.8	52.8	52.8
197	130.1	143.8	130.1	132.5	160.0	132.5	70.0	67.3	67.3	67.3	59.1	72.2	59.1
198	130.1	143.8	130.1	132.5	160.0	132.5	82.9	78.4	78.4	78.4	69.0	76.0	69.0
199	130.1	143.8	130.1	132.5	160.0	132.5	101.3	96.0	96.0	96.0	87.1	99.9	87.1
200	130.1	143.8	130.1	132.5	160.0	132.5	127.4	136.5	136.5	136.5	128.9	113.5	113.5